AFRL-HE-WP-TR-2000-0167

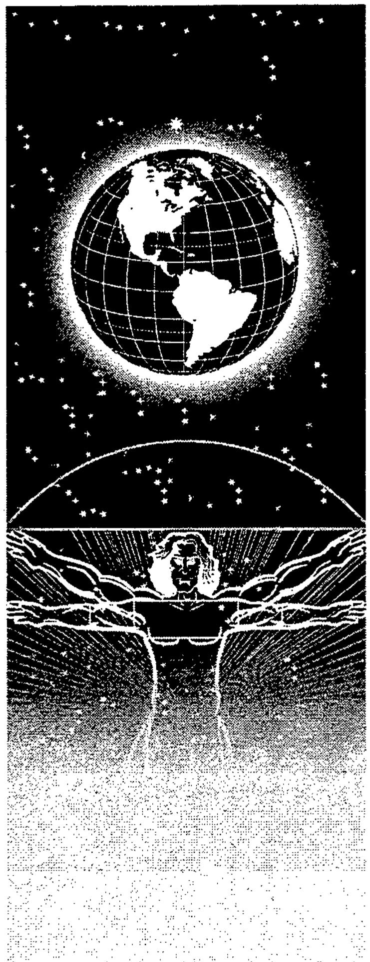

UNITED STATES AIR FORCE RESEARCH LABORATORY

Supersonic Aircraft Noise At and Beneath the Ocean Surface: Estimation of Risk for Effects on Marine Mammals

Hyrum Laney
Raymond C. Cavanagh

SCIENCE APPLICATIONS INTERNATIONAL CORP.
1710 Goodridge Drive
McLean VA 22102

June 2000

Interim Report for the Period October 1996 to April 2000

Human Effectiveness Directorate
Crew System Interface Division
2610 Seventh Street
Wright-Patterson AFB OH 45433-7901

NOTICES

TECHNICAL REVIEW AND APPROVAL

AFRL-HE-WP-TR-2000-0167

This report has been reviewed by the Office of Public Affairs (PA) and is releasable to the National Technical Information Service (NTIS). At NTIS, it will be available to the general public.

This technical report has been reviewed and is approved for publication.

FOR THE COMMANDER

MARIS M. VIKMANIS
Chief, Crew System Interface Division
Air Force Research Laboratory

REPORT DOCUMENTATION PAGE	*Form Approved OMB No. 0704-0188*

1. AGENCY USE ONLY *(Leave blank)*	2. REPORT DATE	3. REPORT TYPE AND DATES COVERED
	June 2000	Interim - Oct 96 to Apr 00

4. TITLE AND SUBTITLE
Supersonic Aircraft Noise At and Beneath the Ocean Surface: Estimation of Risk for Effects on Marine Mammals

5. FUNDING NUMBERS
C - F41624-96-C-9005
PE - 63723F
PR - 2103
TA - C2
WU - C1

6. AUTHOR(S)
Hyrum Laney, Raymond C. Cavanagh

7. PERFORMING ORGANIZATION NAME(S) AND ADDRESS(ES)
Science Applications International Corporation
1710 Goodridge Drive
McLean VA 22102

8. PERFORMING ORGANIZATION REPORT NUMBER

9. SPONSORING/MONITORING AGENCY NAME(S) AND ADDRESS(ES)
Air Force Research Laboratory, Human Effectiveness Directorate
Crew System Interface Division
Aural Displays and Bioacoustics Branch
Air Force Materiel Command
Wright-Patterson AFB, OH 45433-7901

10. SPONSORING/MONITORING AGENCY REPORT NUMBER
AFRL-HE-WP-TR-2000-0167

11. SUPPLEMENTARY NOTES

12a. DISTRIBUTION AVAILABILITY STATEMENT
Approved for public release; distribution is unlimited.

12b. DISTRIBUTION CODE

13. ABSTRACT *(Maximum 200 words)*

This is one of five companion reports, each of which deals with one aspect of the problem of assessing the effects of noise from military aircraft on marine life: metrics for sound properties in air compared to sound properties in water; criteria and thresholds for injury and harassment of protected marine life; animal population statistics; and risks of impact from subsonic/supersonic aircraft noise. The purpose of the effort is to establish technically sound estimation procedures for determining the effects of military aircraft noise on marine life, without which the Air Force risks inadvertent violations of the law and becomes vulnerable to litigation and interference with military operations. Objectives include developing procedures for predicting properties of sound waves in air and under water as generated by both subsonic and supersonic aircraft flights; estimating the effects of sound on marine life, both in air and under water; and determining populations of marine life at risk, as functions of aircraft, flight path, and time of year. This volume specifically focuses on the risks of impact to marine mammals from supersonic aircraft noise.

14. SUBJECT TERMS
acoustics, marine animals, noise impacts

15. NUMBER OF PAGES
44

16. PRICE CODE

17. SECURITY CLASSIFICATION OF REPORT	18. SECURITY CLASSIFICATION OF THIS PAGE	19. SECURITY CLASSIFICATION OF ABSTRACT	20. LIMITATION OF ABSTRACT
UNCLASSIFIED	UNCLASSIFIED	UNCLASSIFIED	UL

This page intentionally left blank.

EXECUTIVE SUMMARY

This is one of five companion reports prepared under the sponsorship of Code HECB of the Air Force Research Laboratory (originally funded by Code AL/OEBN, Armstrong Laboratory of Wright-Patterson Air Force Base). Each of the reports deals with one aspect of the problem of assessing the effects of noise from military aircraft on marine life: (I) criteria and thresholds for injury and harassment of protected marine life, (II)/(III) risks of impact from subsonic/supersonic aircraft noise, (IV) metrics for sound properties in air compared to sound properties in water, and (V) animal population statistics.

The end purpose of this multi-year contract effort is to establish technically sound estimation procedures for determining the effects of military aircraft noise on marine life. Without such procedures, the Air Force risks inadvertent violations of the law and becomes vulnerable to litigation and interference with military operations.

Objectives of the contract effort include developing procedures for:

1) Predicting properties of sound waves in air and under water as generated by both subsonic and supersonic aircraft flights
2) Estimating the effects of sound on marine life, both in air and under water
3) Determining populations of marine life at risk, as functions of aircraft, flight path, and time of year.

This volume specifically addresses the approach to bounding the intensity of the noise field in water generated by a supersonic aircraft. Note here that the propagation mechanisms for aircraft noise into water are completely different for sonic booms because of the limited source angle; this is the reason for a separate volume on the subject.

As explained in Section 2, the properties of noise in water of interest for risk assessment are the peak pressure, modified positive impulse, and energy flux density in selected frequency bands, for each boom event. The number of events over time is also important. Multiple exposure rules vary among precedents and, just as for impact of noise on humans in the work place, may not be simple energy relationships.

Section 3 reviews the well-studied history of propagation of sonic boom noise from air to water, and the behavior of the noise in water. It concludes with a recommended, approximate approach for readily estimating bounds on the metrics of interest. Practicality is emphasized, especially in dealing with the rough surface interface and with propagation of the field in water.

Section 4 provides examples for different aircraft and conditions. It shows the levels of the noise in deep and shallow water. Attention is also paid to the frequency content of the field, since, for example, the majority of marine mammals have very poor hearing at low frequency.

The most important conclusion of this study is that for supersonic flight of Air Force aircraft, there are very few and limited cases for which there might be a compliance issue for noise in

water, under commonly used thresholds. In fact, it is difficult to construct examples for which there is a statistical risk to protected marine life, even for focused booms and exceptionally good propagation across the rough air-sea interface. Such cases can be flagged, and care taken to avoid areas where protected species may be present and at risk [A companion volume, Moore and Clarke (1998), provides this information on marine species at a summary level for training areas, including most of the US coastal region to 200 nmi).

The principal reason for the lack of impact of sonic boom energy under water is that even for the strongest booms and good coupling to the water, the peak pressure and energy flux density are not sufficient to cause injury or harassment, at least under currently accepted criteria and thresholds. As is discussed in the report, an extraordinarily loud boom with peak pressure as great as 50 psf at the water surface will not produce the 12 psi (1700 psf) peak pressure in water associated with harassment of marine mammals and sea turtles. A similar situation applies for energy thresholds.

Nonetheless, estimates of the type made in this volume are essential justifications for arguments of insignificant impact (as would be used in compliance documents or regulator consultations). They also anticipate the event that (as happens every few years) the favored harassment and injury thresholds are changed (from the view of the regulators).

CONTENTS

1.0 INTRODUCTION
- 1.1 First of Series of Five Reports
- 1.2 Organization of Report and Appendices
- 1.3 Acknowledgments

2.0 GEOMETRIES AND METRICS OF INTEREST
- 2.1 Properties of the Noise Field Needed for Risk Assessment
- 2.2 Animal/Interface/Aircraft Geometries

3.0 NOISE ESTIMATION
- 3.1 Sonic Boom Generation and Propagation in Air
- 3.2 Noise Properties at the Air-Sea Interface
- 3.3 Noise Properties across the Interface and in Water
- 3.4 Special Cases: Rough Surface, Focused Booms, Aircraft Maneuvers
- 3.5 Methods for Estimating Noise Properties and for Modifying Existing Noise Models

4.0 EXAMPLES AND CONCLUSIONS
- 4.1 Illustrative Examples of Risk Estimates
- 4.2 Conclusions

5.0 REFERENCES

This page intentionally left blank.

1.0 INTRODUCTION

1.1 First of Series of Five Reports

This is the third in a series of five companion reports prepared under the sponsorship of the Air Force Research Laboratory (AFRL/HECB), Wright-Patterson Air Force Base (originally sponsored by the Noise Effects Branch, Armstrong Laboratory). Each of the reports deals with one aspect of the problem of assessing the effects of aircraft-generated noise on marine life:

Report I: Criteria and Thresholds for Adverse Effects of Underwater Noise on Marine Animals

Report II: Subsonic Aircraft Noise at and beneath the Ocean Surface: Estimation Models for Metrics Associated with Effects on Marine Mammals

Report III: Supersonic Aircraft Noise at and Beneath the Ocean Surface: Estimation Models for Metrics Associated With Effects on Marine Mammals

Report IV: Background Definitions and Metrics for Sound Properties in Air and in Water Relevant to Noise Effects

Report V: Marine Animal Populations for Ocean Regions of Interest to Air Force Flight Operations

The end purpose of this multi-year contract effort is to establish technically sound estimation procedures for determining the effects of military aircraft noise on marine life. Without such procedures, the Air Force risks inadvertent violations of the law and becomes vulnerable to litigation and interference with military operations.

Objectives of the contract effort include developing procedures for:

1) Predicting properties of sound waves in air and under water as generated by both subsonic and supersonic aircraft flights
2) Estimating the effects of sound on marine life, especially under water
3) Determining populations of marine life at risk, as functions of aircraft, flight path, and time of year.

This volume deals with supersonic aircraft noise.

1.2 Organization of Report and Appendices

Section 2 of this report is intended to provide context and motivation for the effort. In particular, it gives examples of the types of information about the noise field that are needed to assess risk to marine life. Perhaps the most important property common to injury and harassment thresholds for protected species is the dependence on exposure time (number of intermittent events).

Section 3 contains a review of the literature on the subject of sound propagation from a source in air to a receiver at or below the air-sea interface. From this review, practical approaches are then recommended for estimating the acoustic field from an aircraft traveling at supersonic speeds. Note that noise from subsonic sources has different propagation physics and is covered in a separate report.

Section 4 gives examples of the time series of sound pressure level that would be observed at a point in the ocean, as generated by a variety of aircraft types and conditions.

An important conclusion is drawn: it would be a rare event for a supersonic aircraft to generate sufficient noise in water to be considered a source of harassment of protected species, at least for commonly used criteria and thresholds. Furthermore, the approach of this volume, combined with data from companion volumes on criteria/thresholds and on mammal/turtle populations, can be used to identify those cases of concern and afford Air Force the opportunity to greatly limit risk.

1.3 Acknowledgments

The authors are pleased to acknowledge the guidance and interest of the sponsor, especially Major Jeffery Fordon, Captain Michael Carter, and Dr. Micah Downing. Special appreciation goes to Robert Lee for his technical support and encouragement throughout.

2.0 GEOMETRIES AND METRICS OF INTEREST

The purpose of this report is not to advance modeling or data analysis technology of aircraft noise in water, but rather quite specifically to provide approaches and examples of how to predict the properties of aircraft noise in water needed to assess compliance risk. The types of noise properties needed for this problem (risk assessment for impulsive noise) include at least three different quantities: peak pressure, energy flux density, and modified positive impulse, with rms pressure an additional possibility. Even these metrics can have complicated constraints, such as "the largest 1/3-octave-band energy level above 100 Hz" from a recent Navy EIS. Some examples are provided below, to help identify what information may be needed and the scales of the problem.

Additionally, geometric relationships among the aircraft, the sea surface, and the marine animals are outlined for context.

2.1 Properties of the Noise Field Needed for Risk Assessment

A companion volume to this report summarizes criteria and thresholds for injury and harassment of protected marine species by underwater noise. Precedents in the eyes of the regulators and other DOD branches (especially Navy and DARPA) must be acknowledged, along with the view of the scientific community.

For impulsive, underwater noise (as for explosives, airguns, and sonic booms), injury and mortality thresholds for marine mammals and sea turtles currently used (and likely to be applicable in the future) are of form:

- peak pressure (including a penalty for multiple exposures),
- energy flux density in a frequency band (also depending on exposure count),
- modified positive impulse (with modification depending on animal depth in water)

Bandwidth modifiers generally reflect the hearing band of the species in question, just as A-weighting is used in evaluating noise impact on humans. There is also the complication of special effects thought to be related to low-frequency sound.

The table below provides some relevant examples of thresholds used in recent compliance work. More on this topic can be found in the companion volume (Cavanagh and Laney, 2000). In the table, decibel quantities for energy flux density are referenced to 1 μPa^2-s.

Table 2-1. Examples of Thresholds

Harassment Criterion	Threshold	Reference
TTS for all small odontocetes	Energy flux density level for band above 100 Hz > 182 dB – 17 log N, where N is number of impulses. Lower threshold limit =120 dB.	SEAWOLF Shock Trial FEIS (1998) and NMFS Final Rule (1998)
Injury for sea turtles	Peak pressure above 15 psi	Young (1991)
Injury for mammals in the form of eardrum rupture	Energy flux density in excess of 1.2 psi-in (205 dB)	SEAWOLF Shock Trial FEIS (1998)
PTS for marine mammals	rms pressure level exceeds 190 dB (re 1 μPa)	HESS committee, as discussed at NMFS criteria workshop (1998)

Here TTS and PTS are degradations in hearing, sometimes treated by regulators as harassment criteria for mammals under the Marine Mammal Protection Act and Endangered Species Act.

To avoid risk or to show that there is no impact, estimates are needed of the relevant properties of noise as received by the animal. Peak pressure and energy in a band are the most common metrics. This paper then provides approaches for estimating these exposure values in the water for the case of supersonic aircraft sources.

2.2 Animal/Interface/Aircraft Geometries

In assessing risk of injury or harassment of protected species, the key elements are the time history of the noise at a site in the ocean (as outlined above) and the movement of the animals of concern. The former is a function of aircraft source level, speed, altitude, and lateral distance, as well as of the propagation environment in air and in water. At each point in the ocean, the time series can be estimated, and the impact assessed. Statistical descriptions of animal populations are then applied to determine the likelihood of encounter.

For multiple exposure potentials, as perhaps from formation flights or multiple explosives, animal motion most also be addressed. The problem often comes down to one of determining the chances that an animal will stay within an area for a specific amount of time. Rather than address the animal motion problem here (it takes many pages), we can only alert the planner to the problem, and note that several methods of solution have been used in the past (see, for example, SEAWOLF (1998) and SSQ-110 EA (1995)).

The usual approach to risk estimation for moving sources and exposure-time-dependent thresholds for injury/harassment is to map out the ocean region consisting of all locations ensonified at or above threshold levels. The expected number of animals affected is then the size of that ensonified region multiplied by animal density. The ensonified region is usually characterized in terms of area, and terms such as 'footprint' or 'sweep region' are sometimes used. If there is a depth bias for the ensonification and the animal location, then the appropriate volume of the region and revised animal densities must be considered.

As an illustrative example, suppose an aircraft ensonifies the ocean region within 1000 m on either side, to depths of 1000 m, at threshold levels (e.g., energy level in excess of 182 dB). If the aircraft follows a non-overlapping path for one hour at 200 km/hr, then the impact region would have area of 200 km^2. If the density of blue whales was 0.0004/km^2, then the expected number of blue whales to be affected would be about 0.08, well below what would ordinarily be considered a significant risk.

3.0 NOISE ESTIMATION

This section reviews the standard references for sonic boom generation and propagation, and then estimates corresponding noise properties at the air-sea interface and in the water column. Noise properties of special interest are peak pressure, pulse duration, "footprint," energy spectrum, and dependencies on aircraft kinematics and receiver depth.

3.1 Review of Features of Sonic Boom Generation and Propagation in Air

Objects moving in the atmosphere at speeds greater than the local speed of sound generate shock waves or sonic booms. In the case of a simple projectile, two primary waves are generated, one at the front of the object and the other at the rear (Figure 3-1). Aircraft present a more complicated picture with waves coming from the bow, air intakes, control surfaces, and tail. At large distances from the aircraft, however, the system of shock waves tends to distort and steepen until they coalesce into a bow and tail wave similar to that from the simple projectile (Figure 3-2).

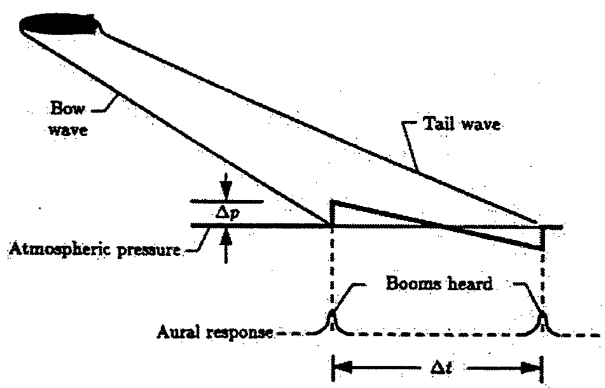

Figure 3-1 Far-field Sonic Boom Pattern (Maglieri & Plotkin, 1995)

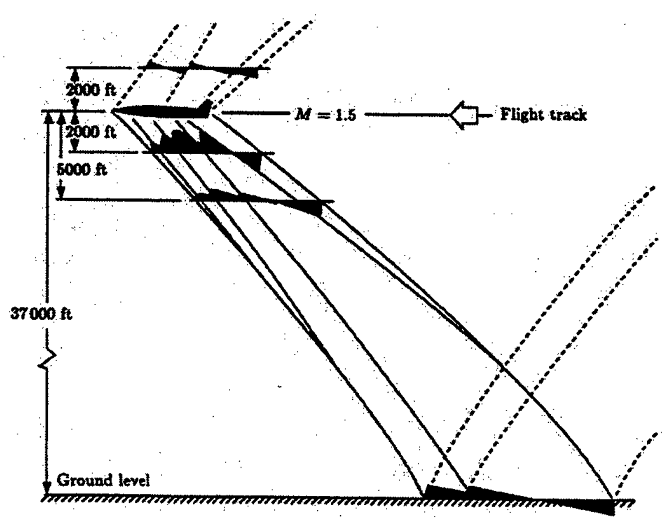

Figure 3-2 Boom Signature as Function of Altitude (Maglieri & Plotkin, 1995)

As the bow wave approaches, the ambient pressure rises quickly to Δp above atmospheric pressure. Following the bow wave a decompression occurs which is corrected with a sudden recompression from the tail wave. Generally the bow and tail waves have similar strength and pressure decreases linearly between the two waves. This sudden compression, linear decompression, and sudden recompression form the classic sonic boom N-wave. N-waves sweep out a sonic boom carpet whose width depends on flight and atmospheric conditions (Figure 3-3). The primary boom is confined to a conical region extending behind the aircraft. The primary boom footprint on the ground is a hyperbolic intersection of the boom cone with the ground (Figure 3-4). The primary boom cone forms an angle of incidence, α, measured from the normal vector to the air-water interface computed as follows:

$$\alpha = \sin^{-1}\left(\frac{1}{M}\right)$$

where M is the aircraft Mach number and M>1 (Figure 3-5). As described in Section 3.3, this angle, known as the Mach angle has value 90° for M=1, 30° for M=2 and approaches 0° as M→∞. For level flight and M<4.35, α is greater than the critical angle (13.3°) for passage of sound from the air to the water and is the most important factor in determining how sonic boom energy couples into the ocean.

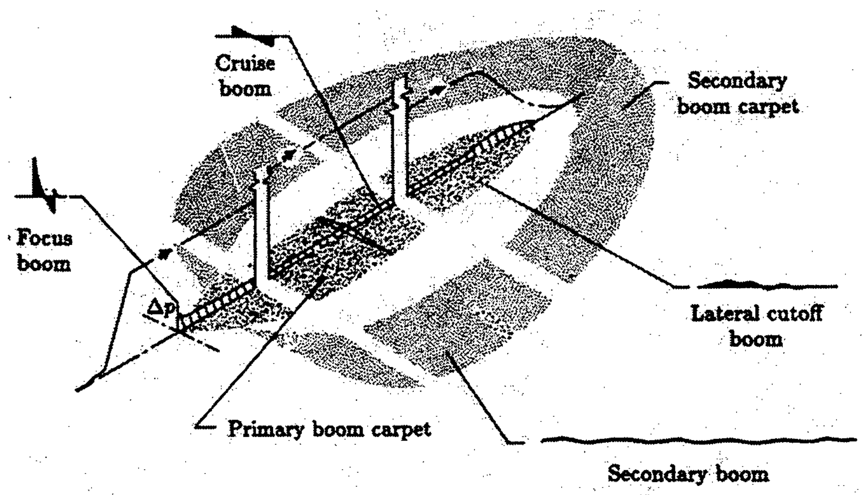

Figure 3-3 Nature of Sonic Boom Ground Exposure (Maglieri & Plotkin, 1995)

Following a supersonic flyby, the observer on the ground may hear two booms in quick succession. The first boom corresponds to the bow wave and the second to the tail wave. For small objects, the two booms may merge into a single detectable event. For aircraft, the time interval between the bow and tail wave is dependent on the length of the airframe, aircraft altitude, and aircraft speed. For most aircraft the time interval is 0.1 seconds or more, allowing the observer to detect two distinct booms.

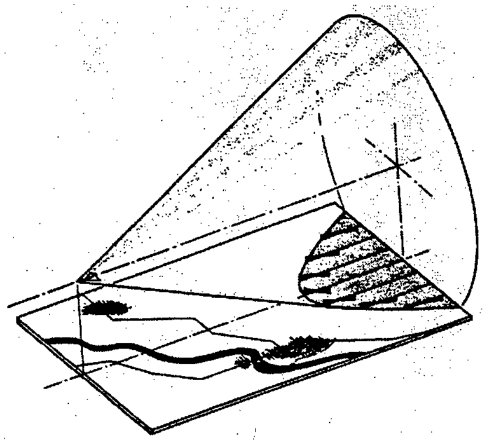

Figure 3-4 Sonic Boom Cone (Carlson & Maglieri, 1972)

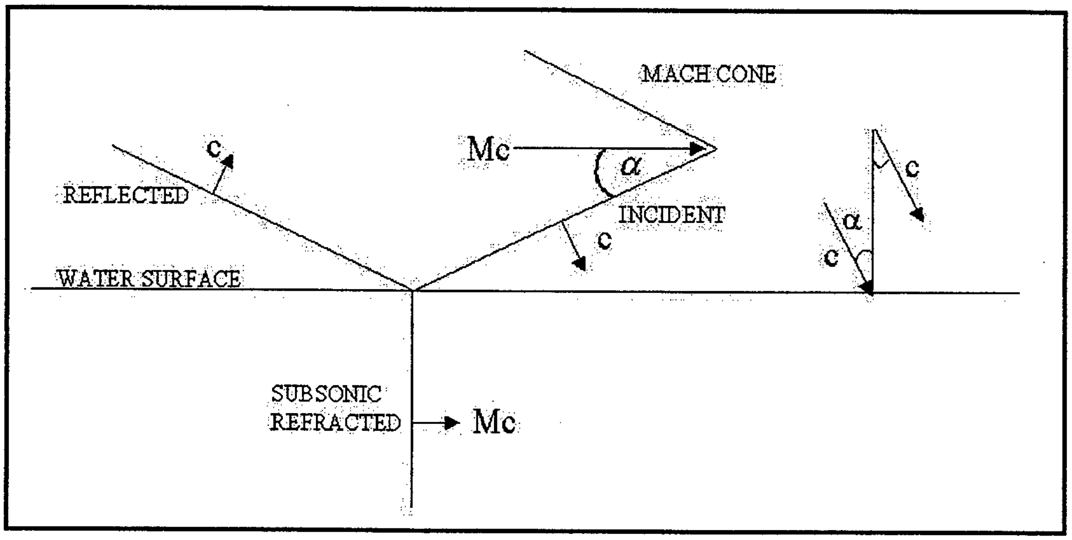

Figure 3-5 Wave and Mach Cone Geometry

In addition to the primary boom carpet characterized by the direct path N-wave, a secondary boom carpet may exist. The extent of the primary boom carpet is limited by the lateral cutoff imposed by the sound speed profile of the atmosphere. Figure 3-6 shows typical wind and temperature profiles for the atmosphere. These profiles limit the range of direct downward path propagation from a source at some altitude to the ground. The secondary boom carpet is formed by waves which either bounce in the region of the primary carpet and are then bent down in the upper atmosphere or by waves which propagate upward and are bent down in the upper atmosphere into the region of the secondary carpet (Figure 3-6). Secondary booms are weak in peak pressure (0.02 – 0.20 lb/ft^2 compared to 0.5- 3.5 lb/ft^2 for typical primary booms) and are in the 0.1 to 2.0 Hz range.

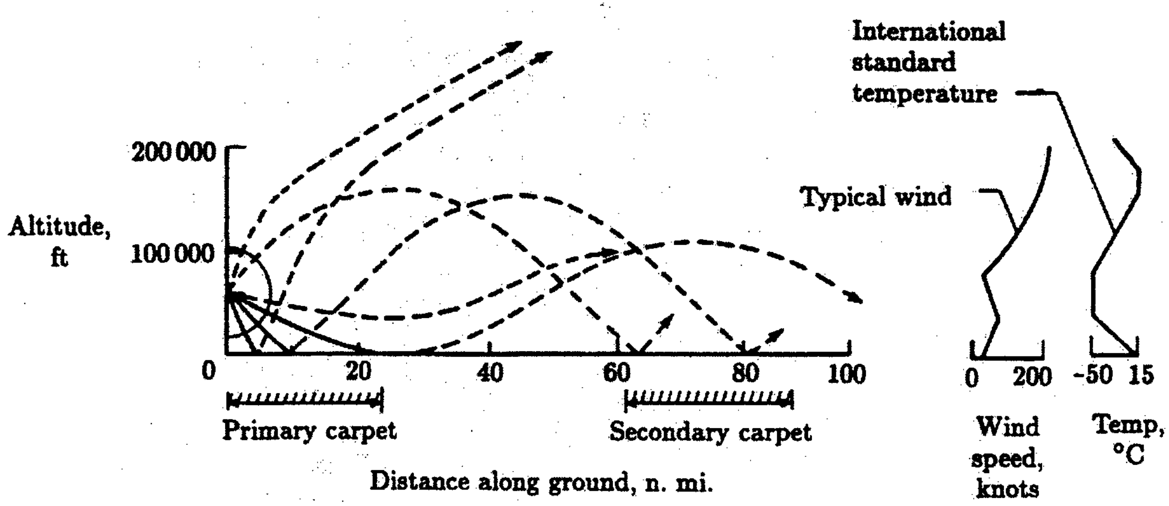

Figure 3-6 Sonic Boom Propagation Paths (Maglieri & Plotkin, 1995)

Variations in the atmosphere also affect the sonic boom signature shape. Turbulence and thermal variations in the lower atmosphere often distort the sonic boom waveform leading to modified N-waves which are peaked or rounded at either the leading or trailing edge of the N-wave or at both ends (Figure 3-7). The categories in Figure 3-7 were developed by NASA and the labels refer to the extent and position of observed "peaking", "spiking", and "rounding". When peaking or spiking occurs, maximum overpressures higher than predicted for a regular N-wave are observed.

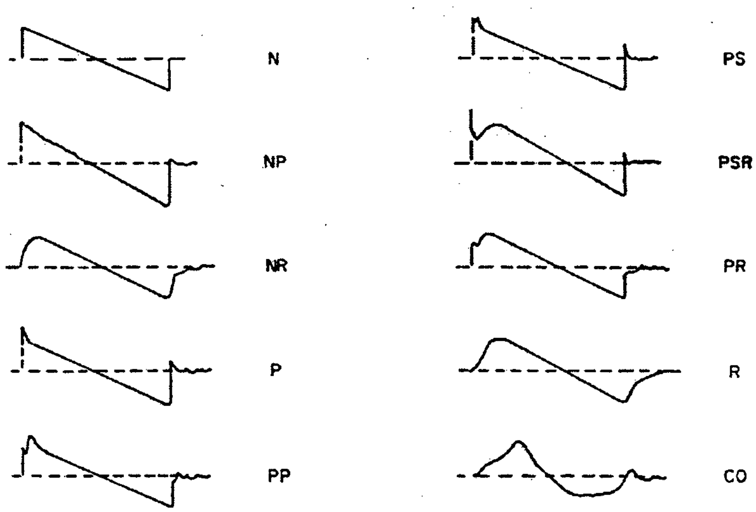

Figure 3-7 Categories of Sonic Boom Waveforms (Pierce, 1968)

3.2 Noise Properties at the Air-Sea Interface

Numerous studies have been conducted to predict and measure the pressure signatures associated with the primary boom carpets produced by objects in supersonic, steady, level flight. For aircraft, the measurements and theory agree with boom levels increasing with aircraft size and decreasing with increasing altitude (Figure 3-8). Peak overpressures for sonic booms are generally in the 0.5- 3.5 lb/ft^2 range and are traditionally expressed in lb/ft^2 in the literature. For reference, a peak pressure of 1 lb/ft^2 is approximately $4.758 \cdot 10^7$ μPa = 47.58 Pa = $6.94 \cdot 10^{-3}$ psi = 153.5 dB (re 1 μPa) = 127.5 dB (re 20μPa).

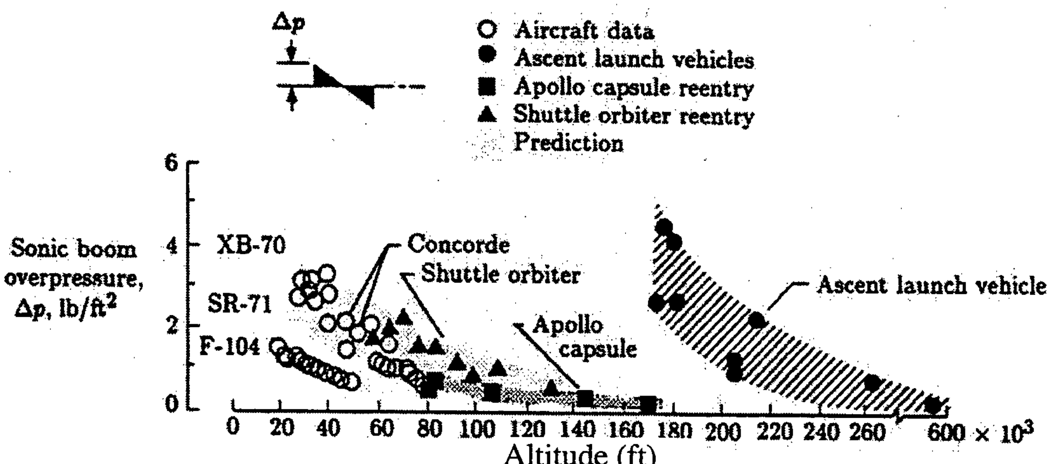

Figure 3-8 Measured and Predicted Overpressures (Maglieri & Plotkin, 1995)

Assuming steady level flight and N-wave arrivals, the following approximations from Carlson, 1978 are generally correct to within 5% of computer calculations (Maglieri & Plotkin, 1995). Carlson also includes approximations for off ground track, climbing, and descending peak pressures which are not presented here. (Note that in Carlson's paper, the units for effective aircraft altitude h_e should be in meters for computing Δp_{max} and Δt.)

$$\begin{aligned} \Delta p_{\max} &= 2K_p K_s \sqrt{P_v P_g}\left(M^2-1\right)^{1/8} h_e^{-3/4} l^{3/4} \\ \Delta t &= K_t \frac{3.42}{c_v} \frac{M}{\left(M^2-1\right)^{3/8}} h_e^{1/4} l^{3/4} K_s \\ P_v &\approx P_g e^{-0.12 \bullet h} \\ K_L &= \frac{W\sqrt{M^2-1}}{1.4 P_v M^2 l^2} \end{aligned} \qquad [1]$$

where

Δp_{max}	shock strength (Pa)
Δt	N-wave duration (s)
P_v	ambient pressure at vehicle altitude (Pa)
P_g	ambient pressure at ground (Pa, nominally 100 kPa)
c_v	speed of sound at aircraft altitude (nominally 300 m/s)
h	aircraft altitude above sea level (km)
h_e	effective aircraft altitude above local ground level (m)

l aircraft length (m)
W aircraft weight (kg (weight))
M aircraft Mach number
K_p pressure amplification factor (see Figure 3-9)
K_s aircraft shape factor (see Figure 3-9)
K_t signature duration factor (see Figure 3-10)
K_L lift parameter (see Equations [1] and Figure 3-9)

The factor of 2 in equation [1] for Δp_{max} is the ground reflection coefficient which is 2 over water. The $\sqrt{P_v P_g}$ factor in equation [1] for Δp_{max} is a partial adjustment for a non-uniform atmosphere (Maglieri and Plotkin, 1995). Equation [1] also accounts for the ray-tube area and aircraft geometry and is based on an $r^{(-3/4)}$ law where r is the equivalent symmetrical body radius.

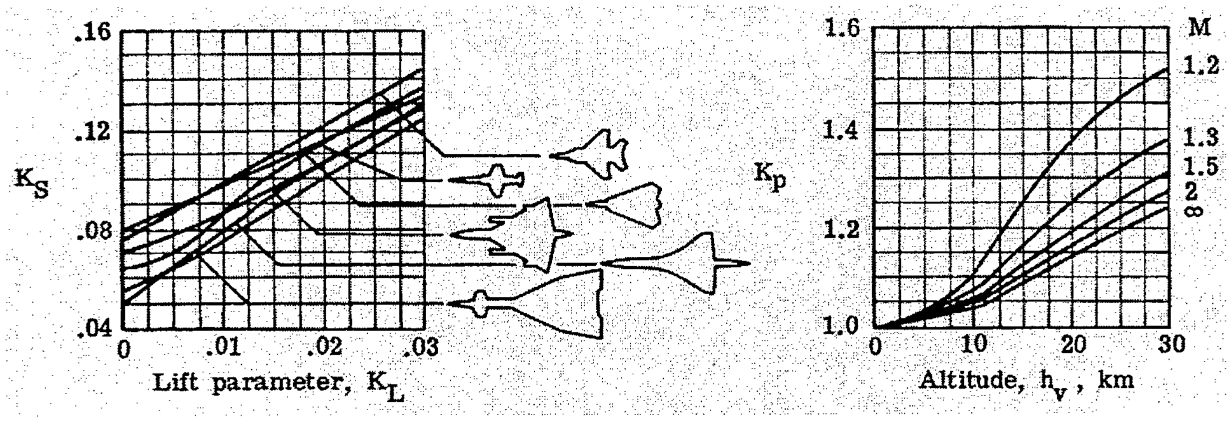

Figure 3-9 Lift and Pressure Amplification Factors (Carlson, 1978)

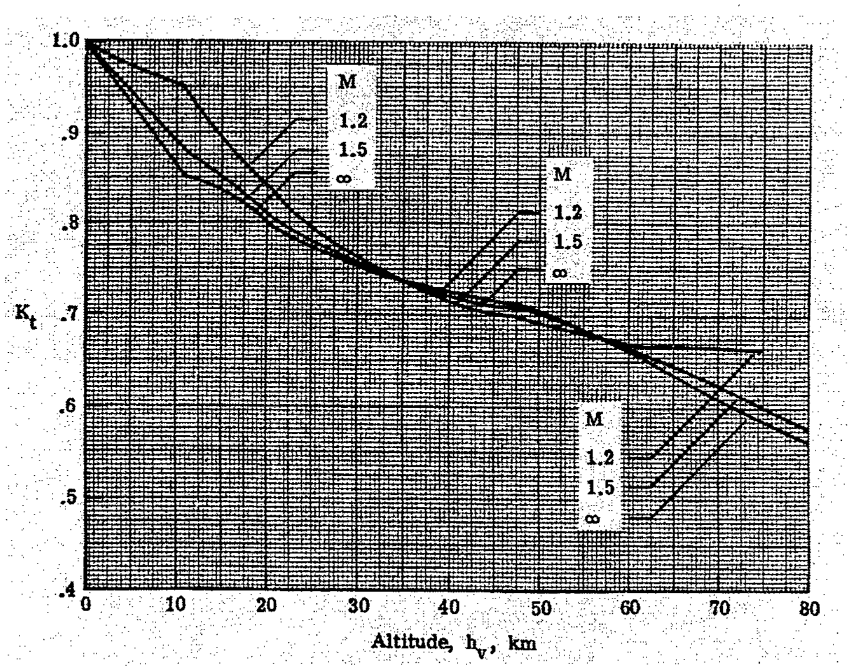

Figure 3-10 Signal Duration Factor (Carlson, 1978)

The power spectrum for an N-wave is computed as follows (Howes, 1967):

$$|P(\omega)|^2 = \frac{1}{(\pi\omega^4 D^2)}\{4 - 4\cos(\omega D) + (\omega D)^2[1+\cos(\omega D)] - 4\omega D\sin(\omega D)\}$$

where ω is sinusoidal frequency and D is the N-wave duration in seconds. Asymptotically the power spectral density changes by 6 dB/octave with positive slope in the low frequencies and negative slope in the high frequencies around the peak (Figure 3-11). It should be noted that the energy spectral density equation presented by Young, 1966 is incorrect. The frequency of the first and dominant peak in the power spectrum is given by Howes, 1967 as:

$$f_{max} \approx 2/(3D).$$

Since typical N-wave durations are 0.035 - 0.3 seconds, typical f_{max} are in the 2 - 20 Hz range. Assuming an 8 Hz peak, the spectrum level at 1000 Hz will be over 40 dB down from the peak spectrum level.

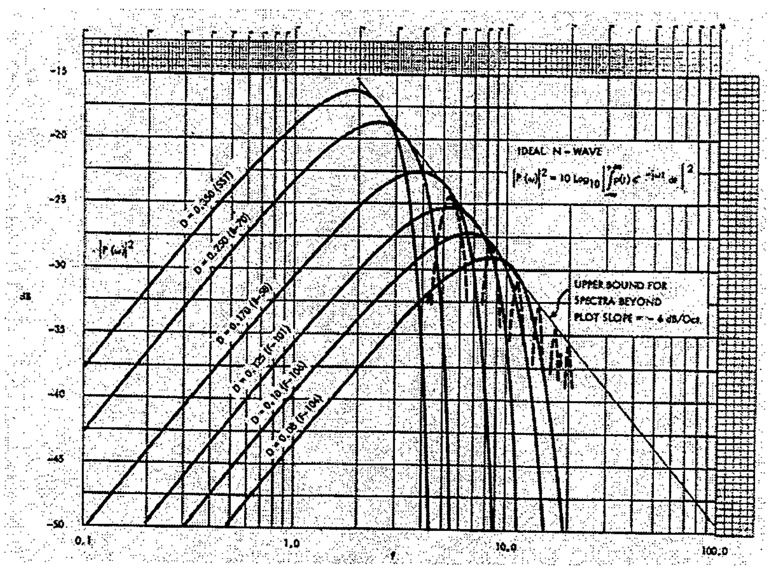

Figure 3-11 First Peak in Power Spectra for Various Aircraft (Young, 1966)

In addition to the peak magnitude and frequency content of a sonic boom, its lateral spread is also of interest. "The extent of the primary carpet is the point at which the ray refracts away from the ground (cutoff distance)" (Magielri & Plotkin, 1995). This cutoff point is determined by the characteristics of the atmosphere, aircraft altitude, and aircraft speed. Figure 3-12 shows boom overpressures as a function of lateral distance from the ground track for an aircraft at an altitude of 60,000 ft traveling in steady level flight at approximately M=2.0. "The widths of the sonic boom carpets on the ground increase with increasing altitude and Mach number" (Magielri & Plotkin, 1995). Figure 3-13 compares the theoretical and measured lateral extent of sonic booms as a function of aircraft speed and altitude. "A crude but useful rule of thumb equates the lateral spread in miles to the airplanes altitude in thousands of feet" (Carlson & Maglieri, 1972).

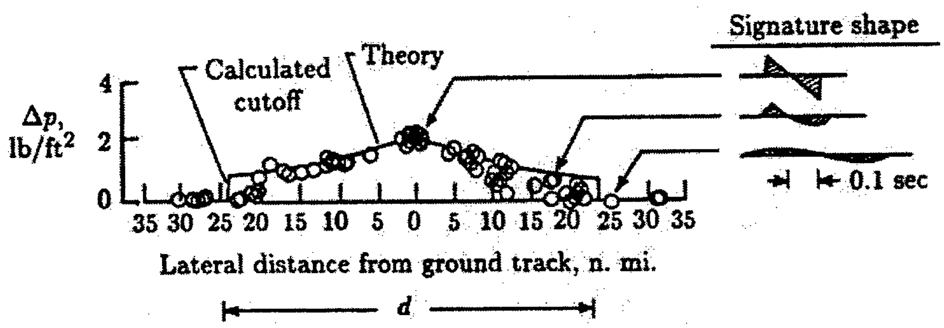

Figure 3-12 Overpressures as a Function of Lateral Distance, M=2 (Maglieri & Plotkin, 1995)

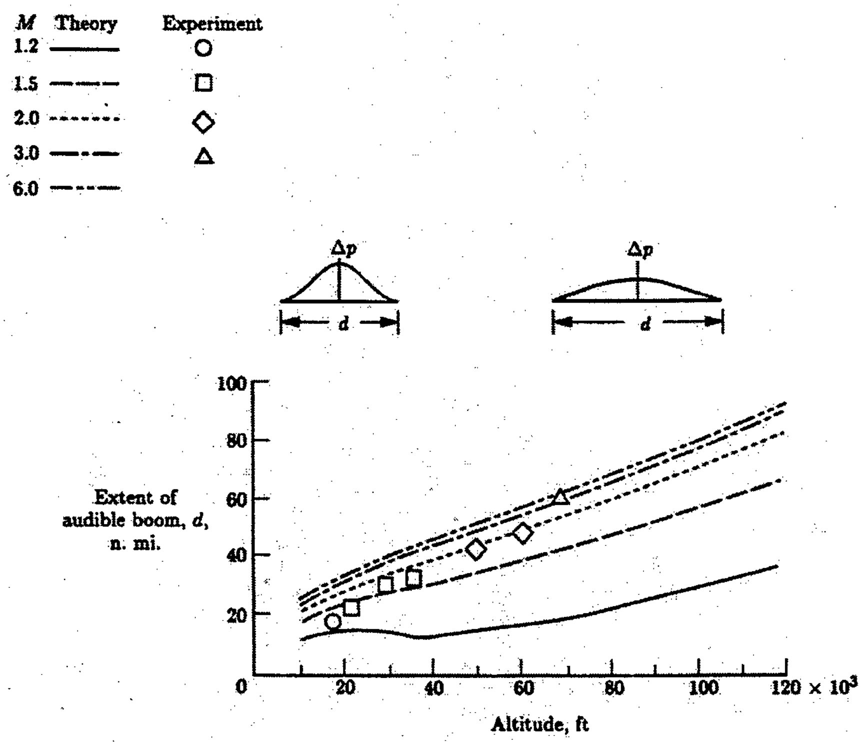

Figure 3-13 Sonic Boom Width on Ground (Maglieri & Plotkin, 1995)

It is useful to summarize what the observer on the ground would experience as the result of a steady level supersonic flyby. An observer directly below the flight path would experience an N-wave, possibly distorted as in Figure 3-7, with a peak pressure and duration which can be estimated using equations [1]. As an observer moves laterally away from the ground track, the signature duration will increase and the peak pressures will decrease as in Figure 3-12. As the observer moves further from the ground track, the signal will disappear as the observer crosses the lateral cut-off defining the primary boom carpet (Figure 3-3). Moving further, an observer would experience the secondary boom carpet where peak pressures are less than 10% of the primary boom peak pressures and where energy is below several Hertz. Typical parameters for a ground observer following a steady level flight are shown in Table 3-1.

Parameter	Primary Boom	Secondary Boom
Peak Pressure (lb/ft^2)	0.5 – 3.5	0.02 – 0.2
Peak Pressure (dB re 20μPa)	121.5 - 138.4	93.5 - 113.5
Wave Duration (sec)	0.035 – 0.3	> 10.0
Wave Shape	N-wave	variable
Boom Carpet Width (nmi)	20 - 60	20 - 50
Mach Angle, α (degrees)	20 - 65	N/A
Peak Frequency (Hz)	2 – 20.0	0.1 - 2.0

Table 3-1 Typical Boom Parameter Values

As with processes such as weathering and corrosion, sonic booms do not generally create instantaneous damage to buildings and other structures but rather contribute to deterioration over time (Warren, 1972). Table 3-2 describes the effect on structures and public reaction to sonic booms with various levels of peak overpressure (Newman and Beattie, 1985).

Peak Overpressure (psf)	Damage to Ground Structures	Public Reaction
0-1	None	None
1-1.5	None	Probable
1.5-1.75	None	Significant (especially at night)
1.75-2.0	None	Significant
2.0-3.0	Incipient	Widespread

Table 3-2 Typical Sonic Boom Damage and Public Reaction (Newman and Beattie, 1985)

3.3 Noise Properties Across the Air-Sea Interface and in the Water

This section addresses the problem of propagation of a sonic boom wave from the air across the air-sea interface into the ocean. Treatments in the literature sometimes appear to be overly complicated, with terms such as the ratio of aircraft speed to sound speed in water (Mach number in water).

In this review, the problem is considered in two parts:

(a) propagation of harmonic plane waves from air to water, the critical angle, and the special case of plane waves arriving at angles shallower than critical angle, and

(b) properties of the sonic boom wave in air at the interface (especially its amplitude, waveform, and arrival angle (Mach angle)), and application of (a) to find the refracted field in water.

Topic (a) is straightforward, and the approach applies to harmonic plane waves in general. The results have been known since at least the time of Rayleigh (Strutt, 1848), and are well explained in the classic textbooks of Officer (1958) and Brekovskikh (1960). The physical principles are quite general, and do not distinguish between sonic booms and other plane waves.

Topic (b), on the other hand, uses the results of (a) and fourier synthesis to estimate the N-wave field in water. The fourier method is routinely used in underwater sound to estimate the propagation of a finite-bandwidth waveform from the properties of the propagation of pure tones, which properties are readily available from popular wave models such as normal mode and parabolic equation models. The fourier approach is older than Rayleigh, and useful explanations for the sonic boom case are given in Sawyers (1968) and Cook (1970). Note that the waveform, amplitude, and arrival angle (Mach angle) are the only properties of the sonic boom used. The Mach number is relevant only in its determination of those properties, and need not appear at all in the formulas for the field in water.

As noted often, the limited impact of sonic boom noise in water is a result of the special coincidence that the Mach angles for most aircraft speeds are not steep enough for good transmission into water. If water had a lower sound speed or airplanes traveled at Mach 5, there would be a significantly greater impact of the sonic boom in water.

3.3.1 Harmonic Plane Wave Reflection and Transmission

From the beginning pages of Brekhovskikh (1960, pp 16 ff), consider the Rayleigh reflection relationships:

$$p_{inc} = A \exp\left(ik_a(x\sin\theta_a - z\cos\theta_a)\right)$$
$$p_{ref} = VA\left(\exp\left(ik_a(x\sin\theta_a + z\cos\theta_a)\right)\right)$$

$$p_w = p_{tr} = WA \exp\left(ik_w(x\sin\theta_w - z\cos\theta_w)\right)$$

where

p refer to the incident, reflected and transmitted pressures,

subscript a is for air and w is for water, c is sound speed, θ is angle (measured from the vertical),

ω is angular frequency

$k = \omega/c$ is wavenumber

$A = -i\rho\omega$ (amp), where amp is the pressure amplitude

and

the frequency factor $\exp(i\omega t)$ has been omitted.

From the boundary conditions of continuity of pressure and continuity of the normal component of the particle velocity across the interface, the Rayleigh coefficients are found as:

$$V = [m \cos \theta_a - (n^2 - \sin^2\theta_a)^{1/2}]/[m \cos \theta_a - (n^2 - \sin^2\theta_a)^{1/2}]$$

$$W = (1/m)(1+V)$$

where

$$m = \rho_w/\rho_a \quad \text{and} \quad n = c_a/c_w = k_w/k_a$$

3.3.2 Plane Wave Propagation form Air to Water, and the Critical Angle.

For propagation from air into water, m has value of about 900 and n about 0.23. Hence, for incidence angles $\theta_a > \arcsin(n) = 13$ degrees, V is a complex number with value close to one (perfect reflection). However, the transmitted pressure in water satisfies:

$$p_w = p_{tr} = WA \exp[ik_w(x\sin\theta_w - z\cos\theta_w)]$$

$$= (1/m)(1+V)A \exp[ik_a x\sin\theta_a + k_a z(n^2 - \sin^2\theta_a)^{1/2}]$$

This corresponds to a wave traveling in the x direction with exponential decay in the z direction. In fact,

$$|p_w| = (2/m)\,|A|\,\exp[-k_a z\,(n^2 - \sin^2\theta_a)^{1/2}]$$

The angle arcsin(n) = 13 degrees is the *critical angle*, so that any plane wave in air that arrives at the air-sea interface at an angle less steep than about 13 degrees will not be transmitted into the water as a propagating wave, but rather as an *evanescent wave*, i.e., one which decays exponentially with depth in the water.

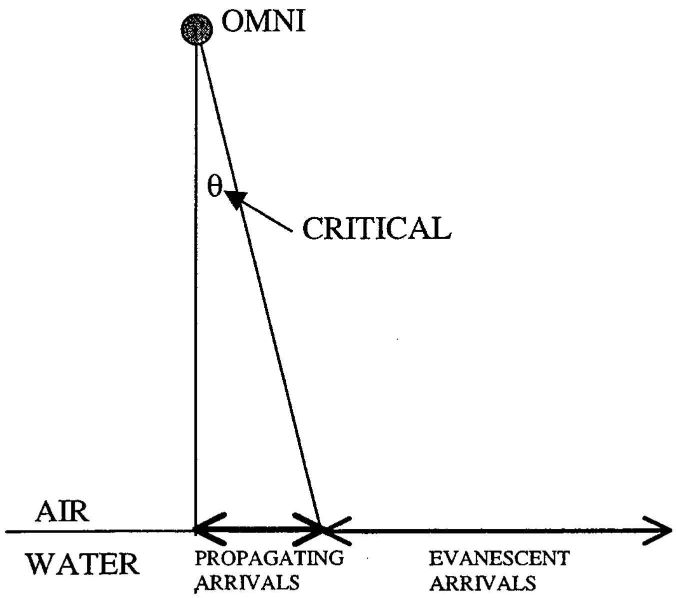

Figure 3-14 Critical Angle Geometry

3.3.3 Application to Sonic Booms – Mach Angle vs Critical Angle

As discussed in section 3.1), an aircraft in level flight at speed Mach M > 1 (i.e., at speed Mc_a) produces a shock wave at the Mach angle ($\alpha = \arcsin(1/M)$). From Figure 3-5, note that this is the angle measured from the axis of the aircraft path, or equivalently the angle that the shock wave makes with the vertical. It is thus the incidence angle of the shock wave at the air-sea interface, and can be compared directly with the critical angle of 3.3.2.

Some sample values of α illustrate that for 1<M<4.3, the incidence angle is less steep than the critical angle, and the wave filed will be transmitted into the water only as an evanescent wave:

M	1.01	1.1	2	3	4.3	6	10
α (degrees)	82	65	30	20	13.1	9.6	5.7

3.3.4 Application to Sonic Booms – Synthesized N-Waves

To finally address sonic boom propagation, begin with an N-wave incident on the air-sea surface at angle α. The results of subsection 3.3.2 apply to harmonic waves (pure tones), but give the pressure field below the interface as a function of arrival angle, position in the water, and frequency.

For aircraft speeds less than about M=4.3, the Mach angle α will be greater than the critical angle. Thus, the incident sonic boom wave in the air is reflected from the surface. The only energy entering the water is in the form of subsonic, non-radiating plane waves whose amplitudes 'evanesce' or decay exponentially with depth below the surface. Air Force manned aircraft fly below M=4 and so all associated sonic booms have only an evanescent transmission into the water.

For an aircraft in constant supersonic level flight over a flat air-water interface, the underwater pressure field generated by a theoretical perfect N-wave can be computed via the fourier-synthesis method mentioned earlier. Following Cook, 1970: "The first step is to find the reflected and refracted waves for an incident sinusoidal wave. The second step is to find the Fourier transform of the incident N-wave, and so to determine the total reflected and refracted waves (caused by the N-wave) by linear superposition of the effects of the incident sinusoidal components". Following this prescription leads to the following underwater sound pressure estimate for an incident N-wave where M < W:

$$\begin{aligned} p_w(x',h) &= 2p_0 \cos\Delta(I_1 \cos\Delta + I_2 \sin\Delta) \\ \pi I_1 &= -\frac{h}{2}\log_e\left[\frac{h^2+(x'+1)^2}{h^2+(x'-1)^2}\right] + x'\tan^{-1}\left[\frac{2h}{h^2-1+(x')^2}\right] \\ \pi I_2 &= \frac{x'}{2}\log_e\left[\frac{h^2+(x'+1)^2}{h^2+(x'-1)^2}\right] + h\tan^{-1}\left[\frac{2h}{h^2-1+(x')^2}\right] - 2 \end{aligned} \qquad [2]$$

where

$$h = \mu z'$$

$$\mu = (1 - M^2/W^2)^{\frac{1}{2}}$$

$$\Delta = \tan^{-1}\delta \approx \delta$$

$$\delta = (\rho/\rho_w)(1 - M^2/W^2)^{1/2}/(M^2-1)^{1/2}$$

x' = scaled horizontal distance from center of N-wave (units of ½ N-wave length)
z' = scaled depth below surface (units of ½ N-wave length)
M = aircraft Mach number
W = ratio of speed of sound in water to that in atmosphere (~4.5)
ρ = density of air (~1.21 kg/m^3)
ρ_w = density of water (~1000 kg/m^3)
p_0 = peak pressure of incident N-wave

The (x,y,z) components of the wavenumber vector for an incident sinusoidal wave are $(k_0,0,k_z)$. The magnitude of this vector is $k=\omega/c$ where c is the speed of sound in air. The same components for the underwater inhomogeneous refracted wave are $(k_0, 0, -iK)$. The complete set of wave numbers (in terms of $k=\omega/c$) for an incident sinusoidal wave is as follows:

$$k_0 = k/M = k\sin\alpha$$
$$k_z = \left(1 - 1/M^2\right)^{1/2} k = k\cos\alpha$$
$$K = \left(1/M^2 - 1/W^2\right)^{1/2} k$$

In terms of (x',y',z') the wavenumbers become:

$$k_0 = k$$
$$k_z = \left(M^2 - 1\right)^{1/2} k$$
$$K = \left(1 - M^2/W^2\right)^{1/2} k$$

where $K/k = \mu$ from equations [2] . The amplitude ratio of the refracted to incident sinusoidal wave for M<W can be written as (Officer, 1958):

$$\frac{2}{\frac{\rho_w}{\rho}\left[1+\delta^2\right]^{1/2}} e^{i\Delta}$$

where Δ from equation [2] is seen to be the phase change between the incident and inhomogeneous refracted wave. Also, the evanescent decay of a sonic boom underwater scales as $e^{-k_0 \mu z'}$ (as shown in section 3.3.2).

For most practical situations $\cos\Delta \approx 1.0$ and $\sin\Delta \approx 0$ so $p_w \approx 2I_1p_0$. For example, if M=1.5 then $\delta=0.001$, $\Delta=0.06$, $\cos\Delta \approx 1.000$ and $\sin\Delta \approx .001$. Given this result, the main part of the sound field is given by $I_1(x',h)$. This function is an N-wave at the surface and spreads out underwater to form infinitely long precursor and tail waves (Figure 3-15). $I_2(x',h)$ has infinite spikes at $x'=\pm 1$, h=0 and also has infinitely long tails and precursors. $I_2(x',h)$ however makes a negligible contribution to the total sound pressure beyond a few centimeters from $x'=\pm 1$ for most cases (Cook, 1970).

Sparrow (1995) points out that equations [2] show that "faster aircraft speeds will produce higher peak pressures at a fixed depth" (all other things being equal, the greater the speed, the steeper the sonic boom arrival). Figure 3-15 shows the normalized pressure resulting from an N-wave on the ocean surface as a function of distance from the center of the N-wave and depth as predicted by equation [2] where M=2.7 . Note that at the ocean surface the peak pressure is twice that of the incident wave in air and that the peak pressure drops by approximately a factor of 8 at a depth of half the N-wave length.

The N-wave travels at approximately M*333m/s where M is the aircraft Mach number. For typical aircraft, N-wave durations are 0.1 – 0.3 seconds leading to underwater exposure times of less that one second.

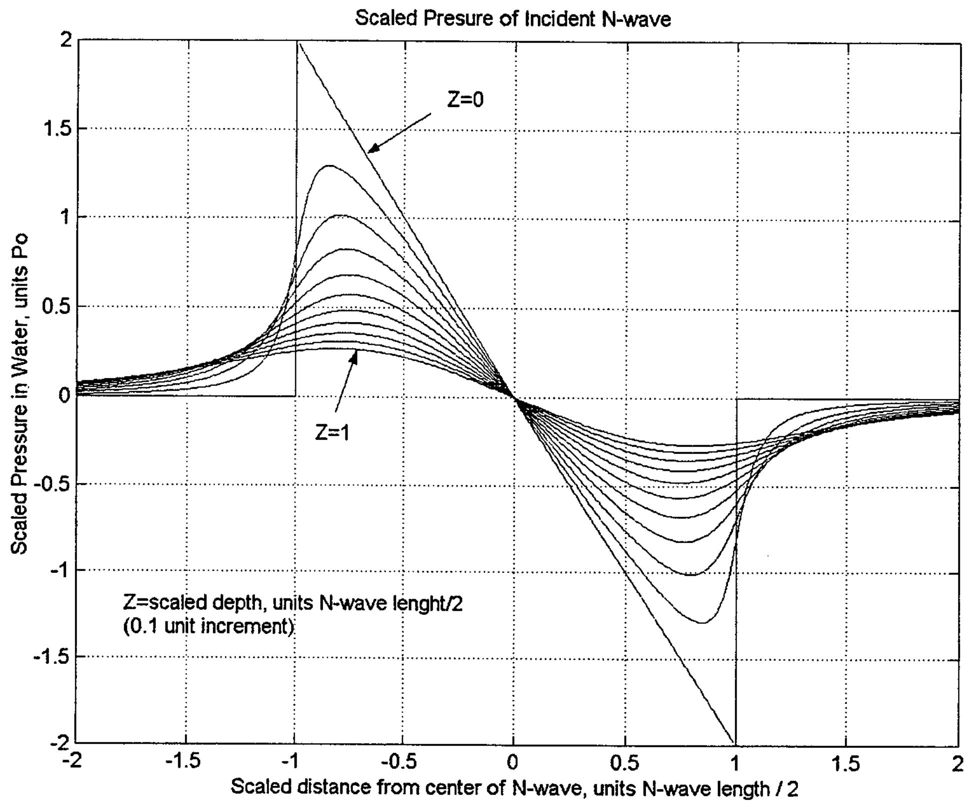

Figure 3-15 Example of Underwater Sound Pressure as Estimated by Equations [2]

As an N-wave penetrates the ocean, high frequency components are quickly attenuated. An example is provided below (Figure 3-16) for an aircraft traveling Mach 2.2 creating a 2.5 psf peak pressure N-wave with a duration of 0.3 seconds. Note that by a depth of 4.6 m, that N-wave pressure levels fall below typical ambient noise levels below 200 Hz. It should be noted that the "typical" ambient levels presented in Figure 3-16 are slightly higher than the values reported by Urick, 1983. Also, the levels presented in Figure 3-16 are spectrum levels.

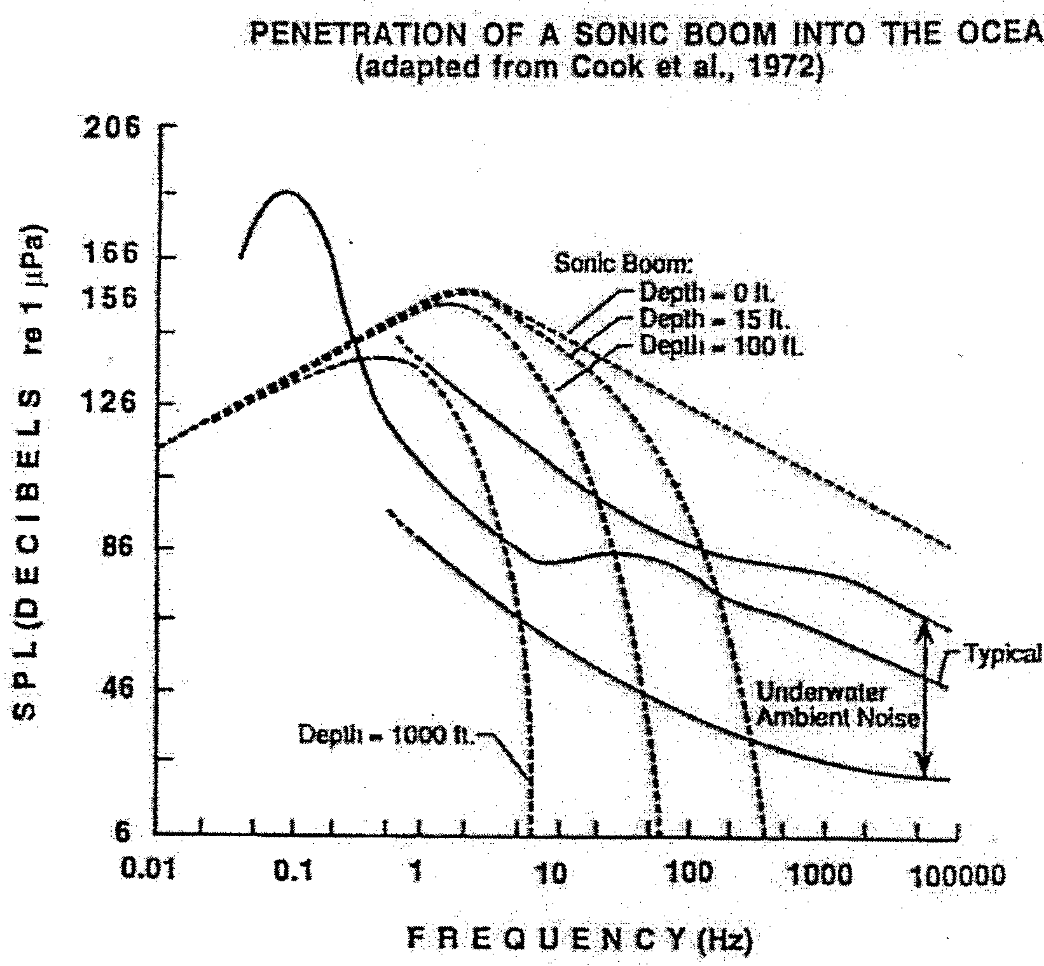

Figure 3-16 Sound Spectra of Sonic Boom at and Below Ocean Surface (Cummings, 1994)

3.4 Special Cases: Aircraft Maneuvers, Focused Beams, Rough Surface

In the case of a diving aircraft, an N-wave arriving at less than the critical angle,θ, can be produced (see Figure 3-14 for geometry). For plane waves incident at angles less than critical, the pressure in the water is approximately twice the pressure of the wave in the air. The transmitted intensity, however, is only about 0.11% of the incident intensity due to the impedance mismatch between the air and water. This corresponds to an intensity decrease of approximately 30 dB. A plane wave with an incident angle θ_A, less than critical, refracts into a plane wave in the water with initial incidence angle θ_W related by $\sin\theta_W = (c_w/c_a) \sin\theta_A$ where $c_{w,a}$ is the speed of sound water and air respectively. Once in the ocean, this wave propagates as a regular plane wave.

Under certain flight conditions, ray paths can converge to form superbooms. Two types of focusing can lead to superbooms. The first is a simple focus corresponding to a caustic. In three dimensions, a caustic is a two dimensional plane which intersects the air-water interface (or ground) in a line. Typical conditions leading to superboom caustic focusing include acceleration and steady turns (Figure 3-17). Caustic peak pressure focus factors of between 2 and 5 have been predicted and observed. Focal boom footprints depend on the maneuver leading to the caustic but are generally confined around the ground track below where the maneuver occurs. The second level of focusing known as superfocusing corresponds to a cusp between two smooth caustics. Superfoci occur during transient maneuvers such as a turn entry. In three dimensions, a superfocus cusp is a line which intersects the ground at a point. Superfoci have been observed with shock focus factors approaching 10 times observed steady level flight N-wave pressures at similar speeds and altitudes. The extent of such superfoci is limited to a few hundred feet in size.

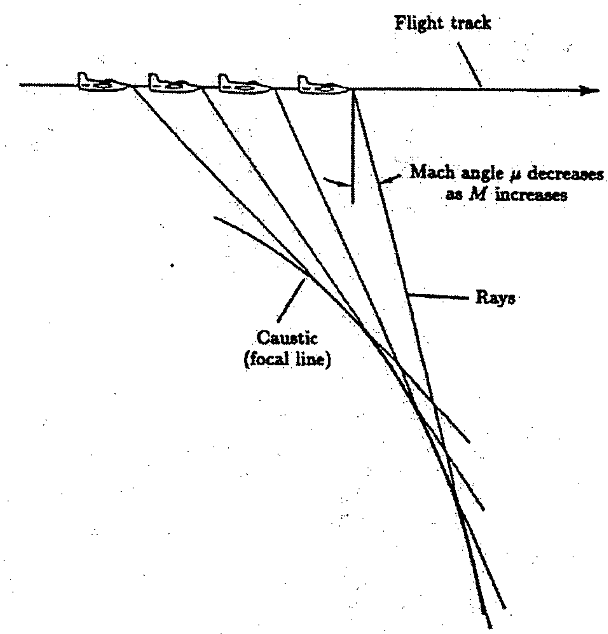

Figure 3-17 Focusing Due to Acceleration (Maglieri & Plotkin, 1995)

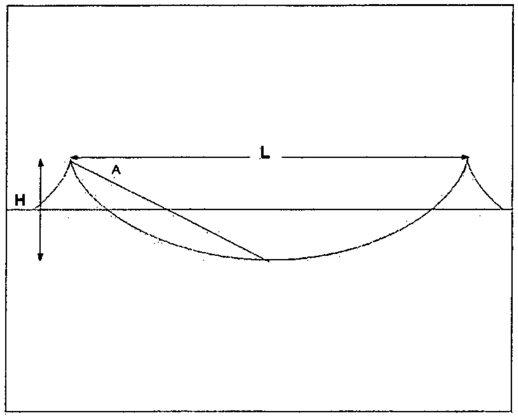

Figure 3-18 Idealized Inverted Cycloid Ocean Wave

All analysis to this point has assumed a flat ocean interface. In the presence of a rough interface, wave slope may allow boom energy to enter the ocean at angles less than critical. Ocean waves can be characterized as inverted cycloids with crest to crest length L and crest to trough height H relative to the still water level. The wave slope can be defined as angle A shown in Figure 3-18. If the difference of the Mach angle $\alpha = \sin^{-1}(1/M)$ and wave slope angle A is less than the critical angle θ=13.3° then boom energy may be injected into the ocean at angles less than critical.

Bowditch (1962) provides tables which relate Beaufort sea state number and fetch in nautical miles to wave height (H in feet) and period (P in seconds) for a fully developed sea. Bowditch also relates the wave length (L in feet) to the period P as : $L = 5.12P^2$.

Using the Bowditch (1962) wave tables and the relationship between P and L, estimates for angle A as a function of sea state and fetch can be computed. Table 3-3 gives estimated wave slopes for fetch distances of 10 and 100 nautical miles for Beaufort numbers between 3 and 10. For reference, Beaufort number 3 corresponds to a gentle breeze, 7-10 knots, while number 10 is described as a whole gale with winds in the 48-55 knot range.

Beaufort Number	Wind Speed (km/h)	Wave Angle (A) in degrees. 10 nmi. Fetch	Wave Angle (A) in degrees. 100 nmi. Fetch
3	12.9 - 19.3	9.1	2.8
4	20.9 - 29.0	10.0	4.6
5	30.6 - 38.6	9.9	5.8
6	40.2 - 50.0	11.5	7.1
7	51.5 - 61.2	11.5	8.2
8	62.8 - 74.0	10.6	9.5
9	75.6 - 86.9	10.5	10.2
10	88.5 - 101.4	12.5	10.8

Table 3-3 Wave Angle Estimates as a Function of Sea State and Fetch

Boom energy will propagate into the ocean if the wave slope angle, A, is greater than angle B = α - 13.3 where α is the Mach angle and 13.3 is the critical angle. Table 3-4 shows angle B as a function of Mach number and shows the sea states where the wave slope, A, is likely to be larger than B thus allowing boom energy to propagate into the ocean at angles below critical.

Mach Number	Angle B (degrees) = α-13.3°	Beaufort Number 10 nmi Fetch	Beaufort Number 100 nmi Fetch
3.5	3.3	>2	>3
3.0	6.2	>2	>5
2.5	10.3	>3	>9
2.0	16.7	>10	>10
1.5	28.5	>10	>10

Table 3-4 Speeds and Sea States Resulting in Boom Waves Below Critical

Table 3-4 indicates that for speeds below Mach 2, ocean slopes leading to propagating boom injection are unlikely for all but the most severe sea states. On the other hand, wave slopes resulting from moderate seas are likely to lead to sub-critical boom angles for aircraft speeds greater than Mach 3. This analysis is supported by Sohn et al., 2000 who conclude "the scattered boom signal is expected to be negligible until vehicle speeds reach Mach ~3. At Mach ~3 very rough sea states have the potential to scatter significant amounts of boom energy into the water column. Between Mach 3 and Mach 4.4 the magnitude of the scattered signal will increase with vehicle speed and sea state."

The recent measurements of Sohn et al. (2000) indicate minimal impact of rough surface effects, and thus support the theory, but only for the case of low sea states and low Mach numbers.

As noted earlier, waves propagating from the air to the water lose about 30 dB of intensity due to the impedance mismatch. Sub-critical propagating waves may also suffer additional losses if the wavelengths of the incident energy are large compared to the length of the ocean waves. Sonic boom energy peaks are in the 2-20 Hz range which corresponds to wavelengths in the 17 - 172 meter range. Based on the tables from Bowditch, 1962, typical surface wavelengths are on the order of 10-30 m for low Beaufort numbers (3-4) and 25-75 m for high Beaufort numbers (8-9) assuming 10–100 nmi fetches. By comparing the acoustic wavelengths associated with the boom energy to those expected for the ocean waves it is apparent that rough ocean coupling losses may be experienced for moderate sea states. Sub-critical wave transmission for a rough ocean is detailed in the companion subsonic aircraft noise report (Eller and Cavanagh, 2000).

3.5 Methods for Estimating Noise Properties

"The United States Air Force is required to analyze the environmental impact from sonic booms produced by supersonic maneuvering aircraft. To meet this, a single event prediction model PCBOOM3 has been developed. This model uses full ray tracing propagation theory and includes the effects of aircraft maneuvers, non-standard atmospheric profiles, and winds. Calculations include focused superbooms when they occur. Input parameters are flexible to allow general supersonic maneuvers. The program accepts user defined F-functions, and has F functions built in for current USAF aircraft. The model predicts the location and waveforms of sonic booms on the ground. Predicted sonic boom footprints are in the form of contours (psf, CSEL, etc) and isopemps, or as tabulated values at specific points." (Plotkin, 1994). The aircraft trajectory is specified by an initial location, altitude, heading, climb angle and first and second derivatives of the Mach number, heading angle, and climb angle. Subsequent positions are projected forward in time using constant second derivatives with an option to change the second derivative with each time advance. The atmosphere is specified by temperature as a function of altitude and wind speed as a function of altitude and direction. The temperature profile is converted into a sound speed profile to which the wind speed profile is added. This method of including wind effects is a standard technique, but treats paths perpendicular to the ground track poorly.

PCBoom3 is used for single sonic boom predictions. "For multiple boom environments, we have two models, CorBoom and BoomMap3. CorBoom predicts the yearly average boom levels, Lcdn, for supersonic operations along a corridor. BoomMap3 predicts the Lcdn contours for supersonic operations in air combat maneuvering instrument areas (ACMI). This program uses the ACMI tracking data to predict the sonic boom environment. Both of these programs used a simplified ray tracing algorithm developed by Dr. Kenneth Plotkin of Wyle Laboratories." (FICAN, 1994).

4.0 EXAMPLES AND CONCLUSIONS

4.1 Examples

Peak pressure and N-wave duration can be estimated using the formulas in equations [1] or computed using PCBoom3. Equations [1] require aircraft length and mass which are summarized in table 4-1 below for several typical aircraft.

Designation	Type	Mass (klbs)	Length (ft)
B-1	Variable Sweep	450	147
F-4	Large Fighter	45	60
F-14	Variable Sweep	55	62
F-15	Fixed Wing Fighter	65	64
F-16	Fixed Wing Fighter	35	49
F-18	Fixed Wing Fighter	39.4	56
F-22	Fixed Wing Fighter	48	67
F-104	Small Fighter	26.5	55
F-111	Variable Sweep	76.5	74
T-38	Small Fighter	20	47
Concorde	Supersonic Transport	387	190
Shuttle	Blunt Lifting Body	187	121

Table 4-1 Selected Aircraft Mass and Lengths (PCBoom3 & WWW)

Equations [1] also require atmospheric pressure, P_v, at the aircraft altitude h. P_v may be crudely estimated using the exponential form presented in [1] or may be taken from more precise measurements. The examples below use pressures from the standard U.S. atmosphere as summarized in Table 4-2 (U.S. Standard Atmosphere, 1976).

Altitude (km)	Pressure (atm)	Pressure (Pa)
0	1.0	101,327
5	0.533	54,021
10	0.261	26,437
15	0.119	12,045
20	0.054	5,475
25	0.025	2,511

Table 4-2 Standard Atmospheric Pressure

Two cases are presented below. The first involves a 450 klb., 147 foot long, B-1 variable sweep wing bomber flying at Mach 1.2. Assume the aircraft is in steady level flight over a flat ocean. The peak pressures and N-wave durations as estimated by Carlson's equations [1] and PCBoom3 are shown in Figure 4-1 as a function of aircraft altitude. The PCBoom3 pressure results were scaled by a factor of 2.0/1.9 to account for the surface reflection factor expected over water (2.0) as opposed to average ground levels (1.9). In general the two models agree, with Carlson predicting slightly higher peak pressures, especially at low altitudes. Figure 4-2 shows peak pressure and N-wave duration variability as a function of Mach number for a B-1 bomber in steady level flight at 10 km altitude. The peak pressure increases about 25% as the aircraft speed increases from M=1.2 to M=3.0. Equations [2] can be used to estimate peak pressures as a function of depth in the ocean. As mentioned earlier, the lateral spread of the primary boom carpet can be estimated by equating the lateral spread in miles to the aircraft altitude in thousands of feet.

For a specific example of a flyover time signature, consider a B-1 bomber traveling at Mach 1.2 at an altitude of 10 km. Based on figure 4-1, the N-wave peak pressure at the air-water interface is 3.7 lb/ft^2 = 164.8 dB which includes the surface reflection factor. The corresponding N-wave duration is 0.325 seconds which for an aircraft speed of 1.2*333m/s leads to an N-wave length of 129.9 m. Using these values, the sound pressure as a function of time from the center of the N-wave and depth is shown in figure 4-3.

The second case study involves a 26.5 klb , 55 foot long, F-104 small fixed wing fighter flying at Mach 2.0. Figure 4-4 shows peak pressure and N-wave duration for a F-104 in steady level flight at Mach 2.0 as a function of altitude. The Carlson and PCBoom models agree very well, with the Carlson peak pressures being slightly higher at low altitudes. Figure 4-5 shows peak pressure and N-wave duration for a F-104 in steady level flight at 10 km altitude as a function of Mach number. As with the B-1 bomber case above, the Carlson N-wave durations fall slightly below the PCBoom3 estimates. Figure 4-6 shows a 10 km altitude, Mach 2.0 F-104 flyover time signature.

Table 4-1 provides N-wave duration, peak pressure and energy flux density level at the ocean surface, 50 m, and 100 m below the surface for a variety of aircraft flying at several altitudes and speeds. The energy density levels, peak pressures, and N-wave durations were computed using the work of Carlson, 1978 (equation [1] and figures 8-9) and Cook, 1970 (equations [2]). Energy density levels were computed by numerical integration where the pressure time series was sampled at Nyquist frequency of at least 1500 Hz. As noted in section 3.2, spectrum levels are at least 40 dB down from their peak above 1000 Hz for surface N-waves. For sonic boom arrivals sampled below the surface, spectrum levels decay faster than the 6 dB/octave seen in the surface N-wave. Therefore, spectrum levels below the surface will be more than 40 dB down from their peak values above 1000 Hz. With this information, the peak and energy density values presented in table 7 can be used for frequencies less than 1000 Hz. Frequencies greater than 1000 Hz will be at least 40 dB lower than the table values.

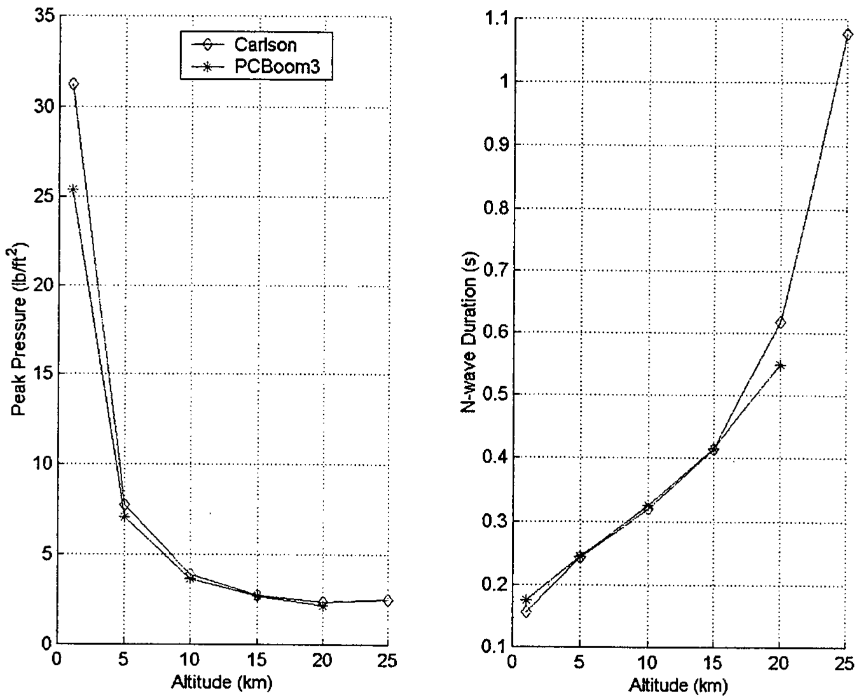

Figure 4-1 B-1 Bomber at Mach 1.2

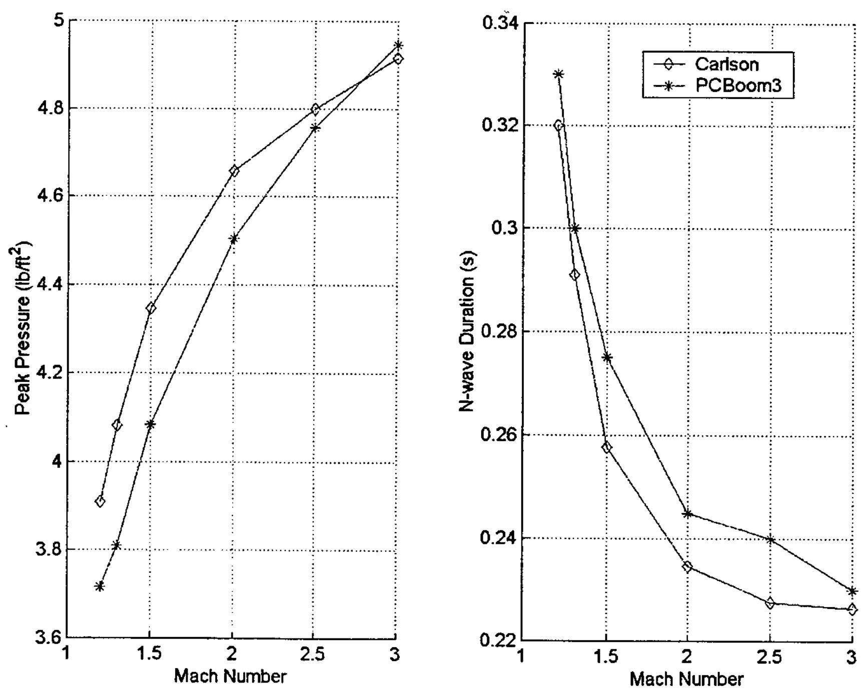

Figure 4-2 B-1 Bomber at 10 km

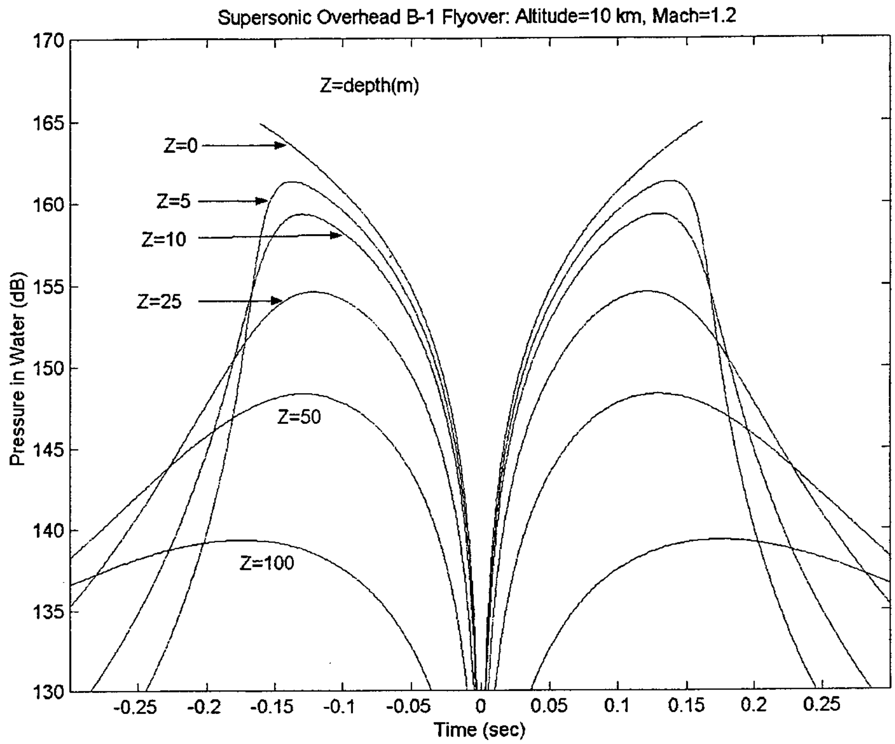

Figure 4-3 Sample B-1 flyover time signature

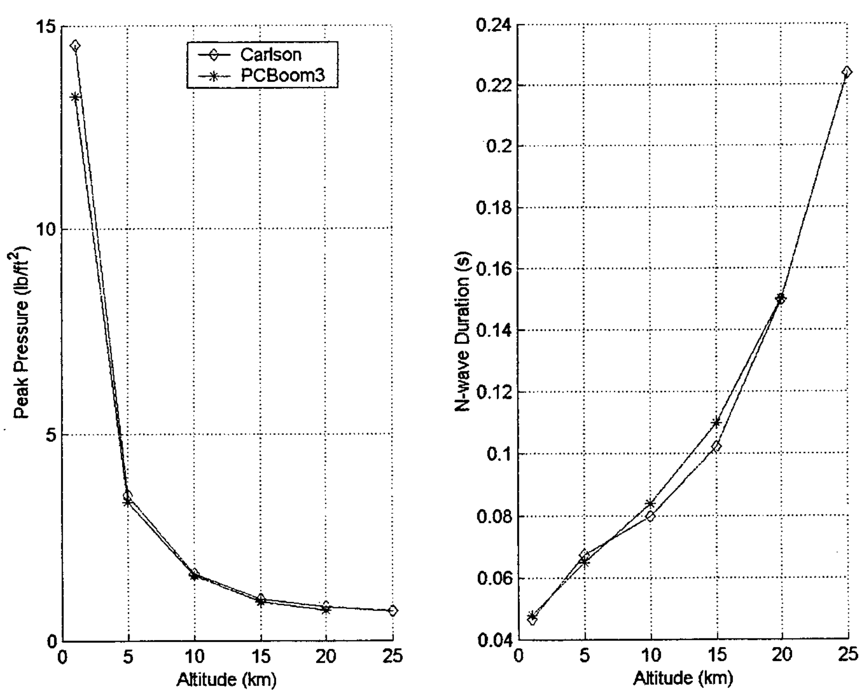

Figure 4-4 F-104 at Mach 2.0

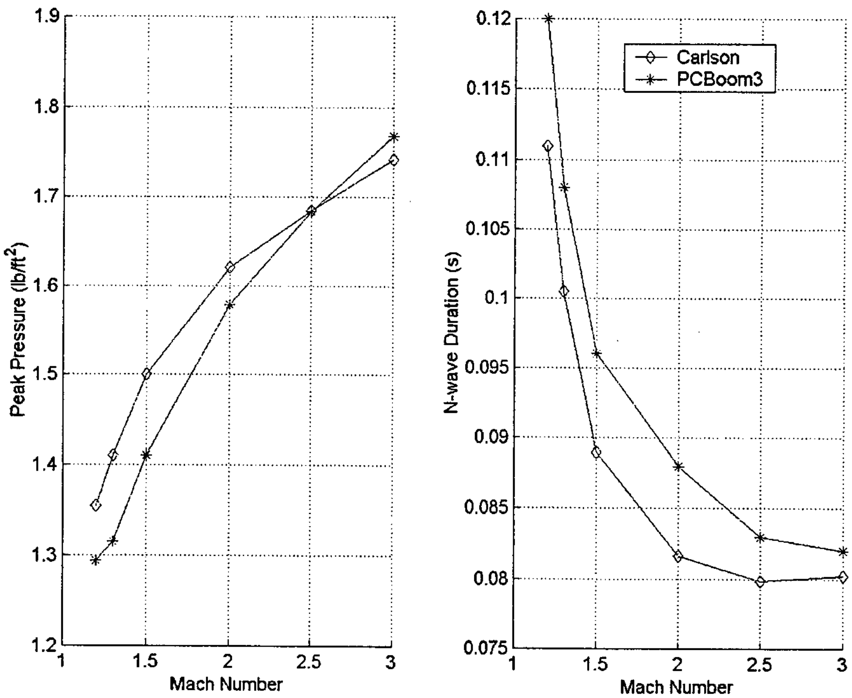

Figure 4-5 F-104 at 10 km

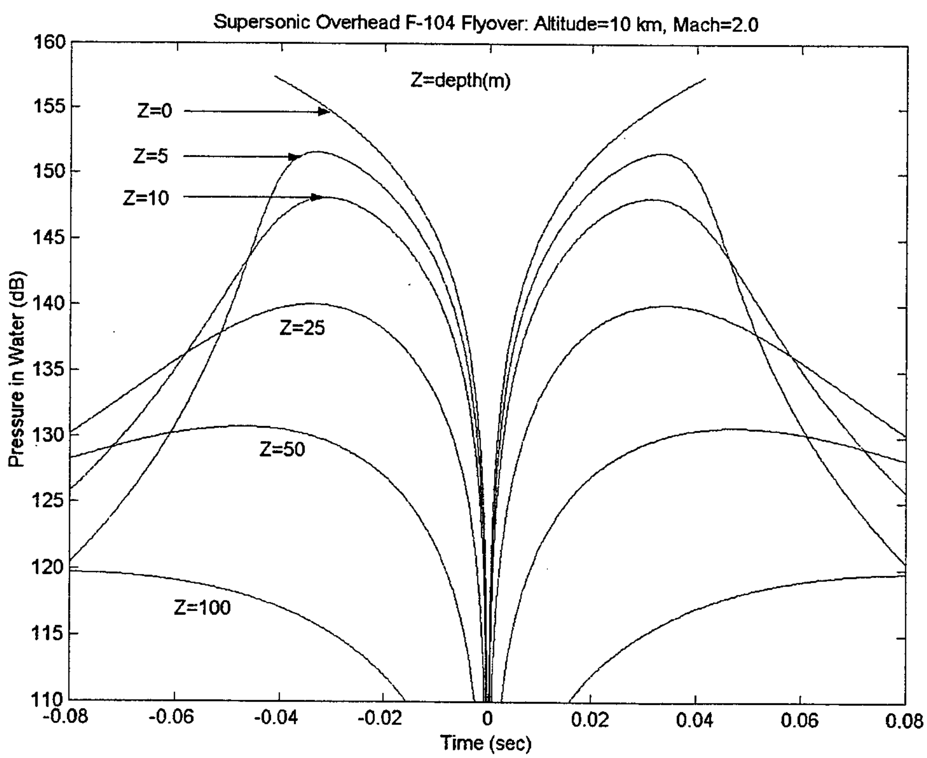

Figure 4-6 Sample F-104 Flyover time signature

MASS (klbs)	LENGTH (ft)	DESCRIPTION	MACH #	ALT (Km)	DURATION (sec)	PEAK PRESSURE (dB)			ENERGY FLUX DENSITY (dB)		
						SURFACE	50 m	100 m	SURFACE	50 m	100 m
20	47	T-38 Talon	1.2	1	0.062	175	134	122	158	127	118
				5	0.094	163	128	117	147	122	113
				10	0.117	156	125	114	142	119	111
35	49	F-16 Falcon	1.2	1	0.066	175	135	124	159	129	120
				5	0.101	163	130	119	148	124	115
				10	0.130	157	128	117	143	122	113
			2	1	0.053	177	143	132	160	135	126
				5	0.077	165	137	120	149	128	120
				10	0.093	159	133	122	143	125	117
40	56	F-18 Hornet	1.2	1	0.072	176	138	126	160	131	122
				5	0.110	164	132	121	150	126	117
				10	0.140	158	130	119	144	124	115
			2	1	0.058	178	146	134	161	137	128
				5	0.084	166	139	128	150	131	122
				10	0.100	159	135	124	144	127	119
48	67	F-22 Raptor (stealth)	1.5	1	0.069	178	143	132	162	136	127
				5	0.102	166	137	126	151	130	121
				10	0.124	160	134	123	146	126	118
			2.5	1	0.066	180	154	143	163	144	136
				5	0.095	167	147	136	152	137	129
				10	0.111	161	142	132	146	132	125
55	62	F-14 Tomcat	1.5	1	0.080	178	145	134	162	138	129
				5	0.101	166	137	126	151	130	121
				10	0.125	160	134	123	146	127	118
			2.5	1	0.065	180	153	142	163	144	135
				5	0.094	167	146	136	152	137	129
				10	0.111	161	142	132	146	133	125
65	64	F-15 Eagle	1.5	1	0.068	178	143	131	162	136	127
				10	0.129	160	134	124	146	127	119
				20	0.259	155	139	130	144	132	126
			2.5	1	0.065	180	154	143	163	144	135
				10	0.114	161	142	133	147	133	126
				20	0.213	155	142	135	143	135	129
387	190	Concord	2	10	0.184	165	148	139	152	141	134
450	147	B-1B Lancer	1.2	10	0.322	165	148	139	155	143	136

Table 4-1 Sonic Boom Levels for Selected Aircraft

4.2 Remarks and Conclusions

At the most fundamental level, consider the acoustic principle for fluids that across any plane the pressure must be continuous (as must be the normal component of the particle velocity). This principle is essential for estimating acoustic propagation from air to water and vice versa, and is invoked in virtually all referenced treatments of the problem. From a practical point of view, it means that twice the pressure in air at the air-sea interface bounds the pressure in the water just below it. Hence a sonic boom of peak pressure 10 psf at the ocean surface becomes an impulsive wave in water with a maximum peak pressure of 20 psf.

The issue then is whether the impulsive wave in the water propagates in depth and range, or not. In most cases of practical supersonic flight, the wave is not a propagating wave, but rather a wave that decays in pressure relatively rapidly in depth or range. As reviewed in Section 3, much research has gone into this problem, including recent work by Sparrow (1995), Rochat and Sparrow (1995), Cheng et al. (1996, 1997), and Sohn et al. (2000), and others.

In some very special cases (e.g., Mach number greater than 4.5, special aircraft maneuvers that momentarily steepen the shock wave angle at the ocean surface, perhaps the case of a very rough sea) sonic boom energy may in fact become propagating energy in water. But again, for practical geometries, twice the pressure at the interface approximates the maximum pressure that will be observed in range or depth.

Now, a very loud sonic boom wave at the ocean surface would be one of order 10 psf. Anything above 50 psf would be difficult to generate (low-flying missiles having been estimated to yield peak pressures on the ground as great as 35 psf). Hence, 100 psf is proposed here as an upper bound that anticipates the worst cases. For comparisons below, note that 100 psf equals about 0.7 psi, or about 194 dB (re 1 μPa).

As discussed at length in the companion volume on thresholds for injury and harassment of marine life (Cavanagh and Laney, 2000), the most commonly used thresholds for harassment of marine mammals and sea turtles by impulsive noise are:

> 12 psi peak pressure, and/or
>
> 182 dB (re 1 μPa^2-s) energy flux density level in the most energetic 1/3 octave band above 10 or 100 Hz (depending on the species).

Thus, even a worst case situation for sonic booms will yield a peak pressure in water well below the 12 psi threshold. As for the energy metric, the calculations in this volume of the energy of sonic boom waves in water yield levels of order 180 dB or less for the 100 psf boom. Table 4-1 can help to put this is perspective.

It is also worthwhile to consider the inverse problem. To approach typical harassment levels for marine mammals, we must have about 12 psi peak pressure in the water. This means that peak pressure of the same order must occur at the surface, in air. But half the pressure in air is 6 psi, or about 900 psf. Note that a sonic boom peak pressure of 50 psf at the ocean surface is considered extraordinary.

For comparison to other impulsive noises in water, consider the standard Navy underwater SUS charge (about 1.8 pounds of TNT equivalent). At 1 meter from the charge, the peak pressure is about 260 dB (re 1 microPa) - about 1000 psi and 144,000 psf. As far away as 1 km, the pressure will be about 1 psi, or 144 psf. To reach the level of a loud sonic boom at the surface (say 10 psf), the observer would have to be about 7 km away. Yet SUS charges are routinely used throughout the world's ocean and assessed by Navy, with agreement of the regulators, as an insignificant risk to protected marine species.

It is evident, then, that by today's standards sonic booms present essentially no risk of harassment for protected marine species in water.

Nonetheless, estimates of the type made in this volume are essential justifications for arguments of insignificant impact (as would be used in compliance documents). They also anticipate the event that (as happens every few years) the favored harassment and injury thresholds are changed (from the view of the regulators). As recently as four years ago, mammal harassment thresholds used in Navy ship shock trials were stated to be as low as 160 dB (energy level). As Table 4-1 indicates, such levels can well occur for selected cases. Detailed risk analyses for specific animal populations and locations would then have to be developed, and mitigation schemes designed to reduce risk.

5.0 REFERENCES

Basset, C. and E. Blanc, "Propagation of Vertical Shock Waves in the Atmosphere," J. Acoust. Soc. Am. **95(4),** 1830-1839 (1994)

Bell, W.B., "Animal Response to Sonic Booms," J. Acoust. Soc. Am. **51**, 758-765 (1972).

Bordelon, D.J., "Sound Pressure in Air from a Source in Water and Vice Versa," J. Acoust. Soc. Am. **55(4)**, 869-870 (1974)

Bowditch, N, *American Practical Navigator*, U.S. Navy Hydrographic Office (H.O. Pub. No. 9), 1966

Bowlanger, P., R. Raspet, H. Bass, "Sonic Boom Propagation through a Realistic Turbulent Atmosphere," J. Acoust. Soc. Am. **98(6)**, 3412-3417 (1995)

Campos, E., and F. Mallen, "Prediction Methods for the Noise Generated by Missiles," Noise-Con 96, 867-872 (1996)

Carlson, H.W., "Simplified Sonic-Boom Prediction," NASA Technical Paper 1122, 1978

Carlson, H.W. and D. J. Maglieri, "Review of Sonic-Boom Generation Theory and Prediction Methods," J. Acoust. Soc. Am. **51**, 675-685 (1972).

Cavanagh, R.C. and J. S. Hanna, "Metrics and standards for acoustic environmental assessments," Invited paper for 129th meeting of the Acoustical Society of America, J. Acoust. Soc. Am. **97**, 3367(A) (1995).

Cavanagh, R. C., "Final Report: Criteria And Thresholds For Adverse Effects Of Underwater Noise On Marine Animals," Science Applications International Corporation, McLean, VA, May 2000

Cavanagh, R. C. and H. Laney, "Final Report: Background Definitions and Metrics for Sound Properties in Air and in Water Relevant to Noise Effects," Science Applications International Corporation, McLean, VA, April 2000

Chapman, D.M., D. J. Thomson, and D. D. Ellis, "Modeling air-to-water sound transmission using numerical codes of underwater acoustics," J. Acoust. Soc. Am. **91**, 1904-1910 (1992).

Chapman, D.M. and P. D. Ward, "The normal-mode theory of air-to-water sound transmission in the ocean," J. Acoust. Soc. Am. **87**, 601-618 (1990)

Cheng, H. K. and C. J. Lee, "Submarine Impact of Sonic Boom: A Study Comparing and Reconciling Result From Two Prediction Approaches," Noise-Con 97, Pennyslvania State University, 15-17 June 1997

Cheng, H. K., C. J. Lee, M. M. Hafez, and W. H. Guo, "Sonic Boom Propagation and Its Submarine Impact: A Study of Theoretical and Computational Issues," American Institute of Aeronautics and Astronautics, 34th Aerospace Sciences Meeting, Reno, NV, 15-18 January 1996

Cook, B.W. and M. J. Lucas, "A Review of Air Force Policy and Noise Models Pertaining to the Noise Environment Under Low-Altitude, High-Speed Training Areas," NOISE-CON 93, 373-377 (1993).

Cook, J.C., Goforth, T. and Cook, R.K., "Seismic and Underwater Responses to Sonic Boom," J. Acoust. Soc. Am. **51**, 729-741 (1972).

Cook, R.K., "Penetration of a Sonic Boom into Water," J. Acoust. Soc. Am. **47**, 1430-1436 (1970)

Courant, R. and K. O. Friedrichs, *Supersonic Flow and Shock Waves*, Interscience, NY (1948).

Cummings, W.C., "Sonic Boom and Marine Mammals: Informational Status and Recommendations," NASA High-Speed Research: Sonic Boom, Volume I (1994).

Dempsey, D.F., "Focusing Conditions for Sonic Booms," J. Acoust. Soc. Am. **61(3)**, 655-658 (1977)

Downing, M., N. Zamot, K. Plotkin, D. Maglieri, "Controlled Focused Sonic Booms from Maneuvering Aircraft," J. Acoust. Soc. Am. **104(1)**, 112-121 (1998)

Eller, A. I. and R. C. Cavanagh, "Final Report: Subsonic Aircraft Noise at and beneath the Ocean Surface: Estimation of Risk for Effects on Marine Mammals," Science Applications International Corporation. McLean, VA, June 2000

Espinosa, A., P. Sierra, W. Mickey, "Seismic Waves Generated by Sonic Booms: A Geoacoustical Problem," J. Acoust. Soc. Am. **44(4)**, 1074-1082 (1968)

Ferguson, B. G., "Doppler effect for sound emitted by a moving airborne source and received by acoustic sensors located above and below the sea surface," J. Acoust. Soc. Am. **94**, 3244-3247 (1993).

Hayes, W.D., and H. L.Runyan, "Sonic Boom Propagation through a Stratified Atmosphere," J. Acoust. Soc. Am. **51**, 695-701 (1972).

Howes, W.L. "Farfield Spectrum of the Sonic Boom," J. Acoust. Soc. Am. **41**, 716-717 (1967).

LGL (1991) - see Richardson et al (1991).

Moore, Sue E. and Janet T. Clarke, "Summary of Marine Mammal Occurrence and Population Estimates in U.S. Coastal Waters Subject to Military Aircraft Overflights," Science Applications International Corporation, San Diego, CA, October 1998

Liszka, L., "Long-Distance Focusing of Concorde Sonic Boom," J. Acoust. Soc. Am **64(2),** 631 (1978)

Lubard, S.C. and P. M. Hurdle, "Experimental investigation of acoustic transmission from air into a rough ocean," J.Acoust. Soc. Am. **60**, 1048-1062 (1976).

Maglieri, D.J. and K. J. Plotkin (Hubbard, H.H. Editor*), Aeroacoustics of Flight Vehicles Theory and Practice (Volume 1: Noise Sources)*, Acoustical Society of America, 1995

Manci, K.M. et al, "Effects of Aircraft Noise and Sonic Booms on Domestic Animals and Wildlife: A Literature Synthesis," U.S. Fish and Wildlife Service, NERC, February 1988.

McNicholas, J.V., "Lateral wave contribution to the underwater signature of an aircraft," J. Acoust. Soc. Am. **53**, 1755 (1973).

Medwin, H. and J. O. Hagy, "Helmholtz-Kirchhoff Theory for Sound Transmission through a Statistically Rough Plane Interface Between Dissimilar Fluids," J. Acoust. Soc. Am. **51**, 1083-1090 (1972).

Meecham, W. C., "High-frequency model for sound transmission from an airborne source into the ocean," J. Acoust. Soc. Am. **60**, 339-342 (1976).

NASA, *High-Speed Research: Sonic Boom*, Volume I, May 12-14, 1993, NASA Conference Publication 10132 (1994).

Naval Air Systems Command (**1995**). "Environmental Assessment for the Use of the AN/SSQ-110 Sonobuoys in Deep Ocean Waters," Enclosure to Navy letter PEO ASW, PMA-264/ ser 060 of 17 March (Confidential Noforn)

Newman, J. S. and K. R. Beattie, "Aviation Noise Effects," Department of Transportation, Federal Aviation Administration, Washington, Report FAA-EE-85-2 (1985)

NRC (National Research Council), "Low Frequency Sound and Marine Mammals, Current Knowledge and Research Needs," National Academy Press (1994).

Officer, C.B., *Introduction to the Theory of Sound Transmission*, McGraw-Hill, 1958

Pestorius, F. M. and S. B. Williams, "Upper Limit on the Use of Weak-Shock Theory," J. Acoust. Soc. Am. **55(6)**,1334-1335 (1974)

Pierce, A. D., *ACOUSTICS, An Introduction to Its Physical Principles and Applications*, Acoust. Soc. Am., Woodbury, NY (1989).

Pierce, A. D. and D. J. Maglieri, "Effects of Atmospheric Irregularities on Sonic Boom Propagation," J. Acoust. Soc. Am. **51**, 722-728 (1972).

Pierce, A. D., "Progressive Wave Equations and Algorithms for Sonic Boom Propagation," NOISE-CON 93, 157-162 (1993).

Pierce, A. D., "Spikes on Sonic-Boom Pressure Waveforms," J. Acoust. Soc. Am. **44(4)**, 1052-1061 (1968)

Plotkin, K. J., "PCBoom3 Sonic Boom Prediction Model-Version 1.0c," Wyle Research Report, Arlington, VA, WR 95-22C (1996)

Plotkin, K. J., M. Downing, and J. Page, "USAF Single Event Sonic Boom Prediction Model:PCBOOM," J. Acoust. Soc. Am. **95(5)**, 2839 (1994)

Plotkin, K.J., "Perturbations Behind Thickened Shock Waves," NASA Third Conference on Sonic Boom Research **SP-255**, 59-66 (1971)

Raspet, R. "Sonic Waves, Blast Waves and Sonic Booms", *Encyclopedia of Acoustics*, Crocker, M. editor, Wiley and Sons, 329-339 (1997)

"Report on Aviation Noise Research Conducted by U.S. Federal Agencies", Federal Interagency Committee on Aviation Noise, 1994

Richardson, W.J., C. R. Greene, C. I. Malme, and D. H. Thomson, "Effects of Noise on Marine Mammals," LGL Ecological Research Associates Inc., Bryan, TX, LGL Report TA834-1, prepared for DOI/MMS, February 1991

Rochat, J.L and V. W. Sparrow, "Sound Levels Under the Ocean Surface Due to Sonic Boom Penetration," Inter-Noise 95, 1995

Rochat, J. and V. Sparrow, "Two-Dimensional Focusing of Evanescent Sonic Boom Noise Penetrating an Air-Water Interface," AIAA/CEAS Aeroacoustics Conference, State College, PA, May 1996

Runyan, L.J. and E. J. Kane, "Sonic Boom Literature Survey," FAA Rept. FAA-RD-73-129-II (Volume 2) "Capsule Summaries." NTIS Number AD771-274 (1973).

Rylander, R. et al, "Experiments on the Effect of Sonic-Boom Exposure on Humans," J. Acoust. Soc. Am. **51**, 790-798 (1972).

Sawyers, K.N., "Underwater Sound Pressure from Sonic Booms," J.Acoust. Soc. Am. **44**, 523-524 (1968).

SEAWOLF Shock Trial FEIS: The "Final Environmental Impact Statement (FEIS) for Shock Testing the SEAWOLF Submarine," Continental Shelf Associates of Jupiter Florida. Department of the Navy, Southern Division, Naval Facilities Engineering Command, P.O Box 190010, North Charleston, S.C. 24919-9010 (May 1998)

Seebass, A. R., *Sonic Boom Research,* NASA Conference Proceedings, SP-147 (1967)

Sohn, R.A. et al., "Field Measurements of Sonic Boom Penetration into the Ocean," J.Acoust. Soc. Am. **107(6)**, 3073-3083 (2000).

Sparrow, V.W., "The Effect of Supersonic Aircraft Speed on the Penetration of Sonic Boom Noise into the Ocean,", J. Acoust. Soc. Am. **97(1)**, 159-162 (1995)

Sonic Boom Symposium, Proceedings, J. Acoust. Soc. Am. **51,** 671-798 (1972).

"SR-71 Experiment on Propagation of Sonic Booms", NASA Tech. Brief, DRC-95-32, 1995

Summary Papers on Human and Animal Hearing Effects in Air: J. Acoust. Soc. Am. **90**, 124-227 (1991).

U.S. Standard Atmosphere, 1976, Government Printing Office, Washington, D.C. , 1976

Urick, R. J., "Noise Signature of an Aircraft in Level Flight over a Hydrophone in the Sea," J. Acoust. Soc. Am. **52**, 993-999 (1972).

Warren, C.H., "Recent Sonic-Bang Studies in the United Kingdom," J. Acoust. Soc. Am. **51**, 783-789 (1972).

Webber, M. and W. Donn, "Ducted Propagation of Concorde-generated Shock Waves," J. Acoust. Soc. Am. **71(2)**, 340-347 (1982)

Young, J. R., "Energy Spectral Density of the Sonic Boom," J. Acoust. Soc. Am. **40**, 496-498 (1966)

Young, R.W., "Sound Pressure in Water from Source in Air," J. Acoust. Soc. Am. **50**, 1392-1393 (1971).

Young, R.W., "Sound exposure level spectra of sonic booms and community noise," in *Proceedings of Inter-Noise 87*, I, 755-762 (1987).

Young, R.W., "Sound pressure in water from a source in air and vice versa," J. Acoust. Soc. Am. **53**, 1708-1716 (1973).